

8

SU-8 Photolithography and Its Impact on Microfluidics

Rodrigo Martinez-Duarte and Marc J. Madou

CONTENTS

8.1 Introduction	231
8.2 SU-8, a Versatile Photoresist.....	233
8.3 SU-8: Photolithography.....	238
8.4 Resist Profiles—An Overview	242
8.5 Choice of Substrate	242
8.6 The Clean Room.....	245
8.7 Substrate Cleaning and Priming.....	245
8.8 Photoresist Deposition	247
8.9 Soft Baking or Prebaking.....	249
8.10 Exposure	250
8.11 Masks and Gray Scale Lithography	252
8.12 Postexposure Bake.....	256
8.13 Development.....	258
8.14 Descumming and Hard Baking	259
8.15 Resist Stripping or Removal.....	260
8.16 Conclusion	261
Acknowledgments.....	261
References.....	262

8.1 Introduction

Microfluidics is the science and technology of systems that process or manipulate small amounts (micro- to picoliters) of fluids, using channels with dimensions of tens to hundreds of micrometers (Whitesides, 2006). Microfluidics offers several advantages in a variety of fields including fuel cells (Dyer, 2002; Jankowski et al., 2002; Erdler et al., 2006; Nguyen et al., 2006; Morse, 2007; Kuriyama et al., 2008; Kjeang et al., 2009), forensics (Verpoorte, 2002), clinical diagnostics (Figeys et al., 2000; Mitchell, 2001; Verpoorte, 2002; Andersson et al., 2003; Verpoorte et al., 2003; Chung et al., 2007), biotechnology (Craighead, 2006), and drug discovery (Weigl et al., 2003; Dittrich and Manz, 2006). An insight into the origin, the present, and the future of this exciting field has been presented by Whitesides (2006). Other excellent reviews are those by Verpoorte et al. (2003), Gravesen et al. (1993), Reyes et al. (2002), Auroux et al. (2002), Dittrich et al. (2006), and Vilknor et al. (2004). The physics and scaling laws in fluidics have been detailed by Beebe et al. (2002), Hu et al. (2007), Janasek et al. (2006), Mijatovic et al. (2005), and Stone et al. (2004). A treatise on the different

dimensionless numbers in microfluidics has been given by Squires and Quake (2005). Although the first reported implementation of microfluidics dates back to ink-jet printers at IBM in the late 1970s (Bassous et al., 1977; Petersen, 1979) and gas chromatographs at Stanford University in the early 1980s (Terry et al., 1979; Tuckerman et al., 1981; Zdeblick et al., 1986), a wider embrace of the technology did not come until the 1990s. In 1990, the term miniaturized total chemical analysis systems, or μ -TAS, was introduced by Manz and colleagues (1990) to refer to the integration of different laboratory steps into a single device, which they projected would range in size from few millimeters to tens of micrometers. In practice, today fluidic platforms might have individual features in that size range, but the whole system is considerably larger. Over the years, the term μ -TAS has been interchangeably used with the term lab-on-a-chip (LOC), although the latter is mostly used to refer to the use of μ -TAS in the healthcare field. LOC-based platforms are expected to effectively diminish the footprint, complexity, and cost of clinical diagnostics and other health-care-related platforms to enable the replacement of centralized, expensive laboratories by point-of-care, portable instruments. To conduct a total analysis, different capabilities must be incorporated into the chip to allow for sample pretreatment, sample separation, selective isolation, and amplification and for the sensing and detection of relevant phenomena. The advantages of such devices include their small size, improved sensitivity, low sample volume requirements, rapid analysis, potential disposability, and most importantly their ease of use that eliminates the need for skilled personnel to perform the assays. The expected impact of this technology on the improvement of global health promises to be highly significant, especially in developing countries where the lack of medical infrastructure is one of the main causes of high mortality rates (Chin et al., 2007). Examples of commercial μ -TAS include the i-STAT[®] portable clinical analyzer by Abbott Point of Care, Inc., the Piccolo[®] Xpress from Abaxis, Inc., and the Apolowako[®] from Wako Diagnostics, Inc.

Microfluidics today relies on the use of different fabrication materials such as silicon, glass, and polymers (Zhang et al., 2006). The first microfluidics devices were fabricated in silicon mainly because microfabrication techniques and materials at that time greatly depended on those used by the integrated circuit (IC) industry. For the ability to optically monitor chemical and biological assays, borosilicate glasses, Pyrex[®], and quartz were soon added to the menu of fabrication materials. The very stable negatively charged surfaces of glasses (silanol groups) also allowed for the implementation of electro-osmotic flow, an electrically induced flow that scales well with miniaturization and offers important advantages over the more traditional flow injection systems (Iverson et al., 2008; Wang et al., 2009). Microfabrication techniques, including wet etching, chemical vapor deposition, and deep reactive ion etching, are commonly used to fabricate silicon-glass microfluidic devices. Significant breakthroughs in gas chromatography, capillary electrophoresis, and other fields have been achieved using these microfluidics devices (Gravesen et al., 1993; Reyes et al., 2002; Jensen, 2006). However, polymers are replacing silicon and glass as the fabrication material of choice for most applications. The wide variety of available polymer compositions, low cost of materials, and relatively inexpensive processing infrastructure enables tailoring the microfluidic substrates/structures to specific applications and allows for disposability (Becker et al., 2000, 2002; Fiorini et al., 2005; Bakajin et al., 2006; Stroock et al., 2006). Commonly used polymers include poly(dimethylsiloxane) (PDMS), poly(methyl methacrylate) (PMMA), polycarbonate, cyclic olefin polymers, polyimide, and epoxies such as SU-8. Other materials include parylene C, Zeonor 1020R[®] (a polyolefin), and polytetrafluoroethylene (PTFE or Teflon[®]). Polymer processing techniques include laser ablation, photolithography, hot embossing, casting, and injection. Perhaps the polymer used mostly in microfluidics research is PDMS, an elastomer that is easily cast. PDMS is an optically clear,

generally inert, nontoxic, nonflammable, porous elastomer that allows for gas exchange, a useful property for cell culturing. It is a hydrophobic material that can be rendered hydrophilic by plasma oxidation (although for short times, only ~0.5 h). Although PDMS is impermeable to aqueous solvents, organic solvents can penetrate the matrix and cause the material to swell (Mata et al., 2005). PDMS microfluidic devices are commonly fabricated on the basis of soft lithography. The latter techniques involve casting PDMS from a master mold and yield affordable processing with fast turnaround times (Duffy et al., 1998b; Xia et al., 1998; Anderson et al., 2000). Despite all its advantages in a research setting, PDMS devices are not yet viewed as strong candidates for commercial applications. Commercial microfluidic platforms are expected to be made from materials such as polycarbonate or cyclic olefin and to be fabricated with techniques such as hot embossing, injection molding, and roll-to-roll processing (Madou et al., 2000). A major problem with polymers as opposed to glasses is their rather low and/or unstable negative surface charges reflected in a difficult-reproduce zeta potential and nonuniform electro-osmotic flow. Different groups have tried to remedy this problem, for example, Locascio and colleagues used polyelectrolyte multilayers* (Barker et al., 2000a, 2000b; Liu et al., 2000) and laser ablation (Pugmire et al., 2002; Henry et al., 2002) to modify the surface of different polymers including polystyrene, poly(ethylene terephthalate) glycol, PMMA, polyvinyl chloride, polycarbonate, and PDMS. PDMS is commonly rendered hydrophilic using oxygen plasma, but other available methods for surface modification include ultraviolet (UV)/ozone oxidation (Berdichevsky et al., 2004) and surface coatings, for example, the use of a three-layer (biotinylated IgG, neutravidin, and biotinylated dextran) biotin–neutravidin sandwich (Linder et al., 2001). A review on the zeta potential of different polymer substrates is given by Kirby et al. (2004a, 2004b). Sikanen et al. (2005) characterized the zeta potential on SU-8 surfaces and observed an electro-osmotic flow equal to that for glass microchannels at $\text{pH} \geq 4$.

Although SU-8 is currently the material of choice to fabricate casting molds for PDMS, the authors believe that SU-8 has not yet been fully exploited as a structural material for microfluidics. For example, although SU-8 offers several advantages for the fabrication of structures of high aspect ratio, its processing parameters require further characterization. In this chapter, we detail the photolithography process to fabricate SU-8 structures with dimensions ranging from millimeters to hundreds of nanometers. In the first section, the reader will get acquainted with the origin and properties of SU-8 as a material and why it is so useful in microfluidics. The section “SU-8, a Versatile Photoresist” details all the fabrication steps in the SU-8 photolithography process and presents optimization tips so that one might be able to better exploit the potential of this versatile material. As previously noted, we emphasize SU-8 photolithography that results in either better molds or permanent structural elements in better-functioning microfluidic devices.

8.2 SU-8, a Versatile Photoresist

To understand the photolithographic process better, we start detailing the photoresist. The principal components of a photoresist are a polymer (base resin), a sensitizer, and a casting solvent. The polymer changes structure when exposed to electromagnetic radiation, the

* Multilayers are created by exposing a surface to alternative solutions of positively and negatively charged polyelectrolytes.

solvent allows for spin-coating uniform layers on a flat substrate, and the sensitizers control the photochemical reactions in the polymeric phase. Photoresists must meet several rigorous requirements: good adhesion, high sensitivity, high contrast, good etching resistance (wet or dry etching), good resolution, easy processing, high purity, long shelf life, minimal solvent use, low cost, and high glass transition temperature, T_g . Most resins, such as novolacs, used as a basis for photoresists are amorphous polymers that exhibit viscous flow with considerable molecular motion of the polymer chain segments at temperatures above the glass transition point. At temperatures below T_g , the motion of the segments is halted, and the polymer behaves as a glass rather than a rubber. If the T_g of a polymer is at or below room temperature, the polymer is considered a rubber; if it lies above room temperature, it is considered to be a glass.

SU-8 is an acid-catalyzed negative photoresist,* made by dissolving EPON® SU-8 resin (a registered trademark of Shell Chemical Company) in an organic solvent such as propylene glycol methyl ether acetate (PGMEA), cyclopentanone, or gamma-butyrolactone (GBL) and adding up to 10 wt% of triarylsulfonium hexafluoroantimonate salt as a photoinitiator. Commercial formulations also include 1%–5% propylene carbonate. In a chemically amplified resist such as SU-8, one photon produces a photoproduct that, in turn, causes hundreds of reactions to change the solubility of the film. Because each photolytic reaction results in an “amplification” via catalysis, this concept is dubbed “chemical amplification” (Ito, 1996). The viscosity of the photoresist and hence the range of thicknesses accessible are determined by the ratio of solvent to SU-8 resin. The EPON resist is a multifunctional, highly branched epoxy derivative that consists of bisphenol-A novolac glycidyl ether. On an average, a single molecule contains eight epoxy groups that explain the 8 in the name SU-8 (Figure 8.1). The material has become a major workhorse in miniaturization science because of its low UV absorption (up to thicknesses of 2 mm), high chemical and thermal resistance, and good mechanical properties that make it suitable as a structural material. For example, Abgrall et al. (2007) fabricated SU-8 microfluidic devices with different techniques, including the successive lamination and patterning of SU-8 layers on existent topographies. The use of SU-8 photoresists allows for the coating of thick layers (up to 500 μm) on a single spin coat, or thicker layers in multiple spin coatings, and high-aspect-ratio structures with nearly vertical side walls.

SU-8 cross-linking starts upon the irradiation of the photoresist. In the exposed areas, the photoinitiator decomposes to form hexafluoroantimonic acid that protonates the epoxides on the oligomer. These protonated oxonium ions are, in turn, able to react with neutral epoxides in a series of cross-linking reactions after application of heat. In other words, irradiation generates a low concentration of a strong acid that opens the epoxide rings and acts as a catalyst of the chemically amplified cross-linking process that gets further activated by the application of heat.

On the basis of discoveries in the late 1970s by Crivello and Lam at General Electric (Crivello et al., 1977, 1979, 1980; Crivello, 2000), scientists at IBM discovered that certain photoinitiators, such as onium salts, polymerize low-cost epoxy resins such as EPON-SU-8. Compositions of SU-8 photoresist were patented by IBM as far back as 1989 (Gelorme et al., 1989) and 1992 (Angelo et al., 1992). Originally, SU-8 was intended for printed circuit board and electron beam lithography (EBL), but it is now used in a wide variety of

* If the photoresist is of the type called *negative* (also *negative tone*), the photochemical reaction strengthens the polymer by random cross-linkage of main chains or pendant side chains, thus becoming less soluble. If the photoresist is of the type called *positive* (also *positive tone*), the photochemical reaction during exposure of a resist weakens the polymer by rupture or scission of the main and side polymer chains, and the exposed resist becomes more soluble in developing solutions. In other words, in negative photoresists light cross-links, whereas in positive ones light scissions.

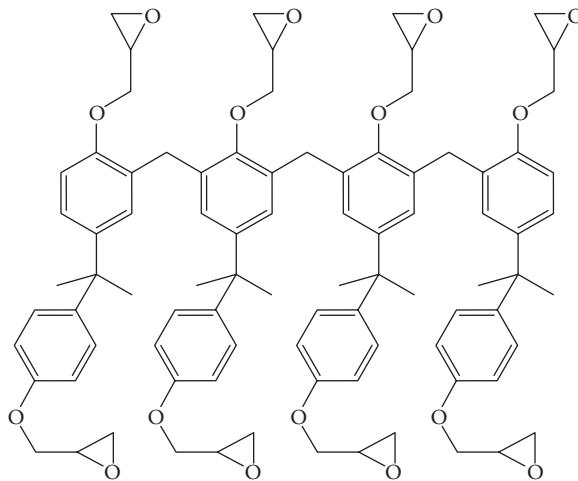


FIGURE 8.1
The SU-8 molecule.

other processes (Lee et al., 1995; Lorenz et al., 1997, 1998; Shaw et al., 1997). In view of the many advantages of SU-8 photoresists over available UV photoresists, including the fabrication of high-aspect-ratio microelectromechanical system (MEMS) features, different formulations of SU-8 photoresists began to be commercialized by MicroChem in 1996. Because of its aromatic functionality and highly cross-linked matrix, the SU-8 resist is thermally stable and chemically very inert. When fully polymerized, it withstands nitric acid, acetone, and even sodium hydroxide (NaOH) at 90°C, and it is more resistant to prolonged plasma etching and is better suited than PMMA as a mold for electroplating (Harris, 1976). The low molecular weight ($\sim 7000 \pm 1000$ Da) and multifunctional nature of an epoxy gives it a high cross-linking propensity, which reduces the solvent-induced swelling typically associated with negative resists. Very fine feature resolution, unprecedented for negative resists, was obtained, and as a result epoxy-based formulations are now used in the fabrication of high-resolution semiconductor devices and nanofluidics. For example, nanochannels can be fabricated using EBL for a variety of applications as suggested by Koller et al. (2009) and Gersborg-Hansen et al. (2006). Low molecular weight characteristics also translate into high contrast and high solubility. Because of its high solubility, very concentrated resist-casting formulations can be prepared. The increased concentration benefits thick film deposition (up to 500 μm in one spin-coating step) and planarization of extreme topographies. The high epoxy content promotes strong SU-8 adhesion to many types of substrates and makes the material highly sensitive to UV exposure. From the microfluidics point of view, strong adhesion to the substrate and chemical inertness of the SU-8 are very desirable. In contrast, the same two properties make resist stripping a very challenging problem for those applications where the resist must be removed such as in the IC industry. Stripping of SU-8 may be carried out with hot NMP (1-methyl-2-pyrrolidone), plasma, laser ablation, or simple burning (Dentinger et al., 2002).

Previously, we listed several benefits of the SU-8 photoresist. Here, we analyze some of the negative aspects such as the thermal mismatch between SU-8 and common substrates such as Si or glass, which produces stress and may cause film-cracking. Also, the

absorption spectrum of SU-8 shows much higher absorption coefficients at shorter wavelengths and as a result, lithography, using a broadband light source, tends to result in overexposure at the surface of the resist layer and underexposure at the bottom of the resist layer. The exaggerated negative slope at the top of the resist structure's surface is often called *T-topping*. UV light shorter than 350 nm is strongly absorbed near the surface's creating locally more acid that diffuses sideways along the top surface. Selective filtration of the light source is often used to eliminate these undesirable shorter wavelengths (below 350 nm) and thus obtain better lithography results.

In Table 8.1, we list some of the most important properties of SU-8. Data sources for the properties SU-8 of listed here (and many more) can be found in Chollet (2009) and Guerin (2005).

The appearance of SU-8 is pale yellow to clear, and it has a faint to mild odor. The mechanical properties of cross-linked SU-8 listed in this table include a Young's modulus ranging from 4.02 to 4.95 GPa, a Poisson ratio of 0.22, and a friction coefficient of 0.19. The glass temperature, T_g , of the unexposed resin ranges from 50°C to 55°C but increases to >200°C when it is fully cross-linked. This allows for the use of SU-8 structural elements in microfluidics applications where heating is necessary, such as polymerase chain reaction assays (where the sample temperature must be increased to 98°C). The degradation temperature, T_d , is ~380°C. Other thermal properties listed here include a coefficient of thermal expansion (CTE) of $52 \times 10^{-6}/\text{K}$ and a thermal conductivity of 0.2 W/m K. SU-8, the EPON resin not the photoresist, features a density of 1200 kg/m³. Cross-linked SU-8 features a refractive index of 1.67–1.8 and a relative dielectric constant of 4–4.5 depending on the frequency. Unexposed SU-8 has a refractive index of 1.668 at 365 nm wavelength. As previously noted, the viscosity of the different commercial photoresists depends on the resin to solvent ratio. Table 8.2 lists the viscosity values, percentage of solids, and

TABLE 8.1

Selected Properties fo SU-8

Appearance	Pale yellow to clear
Odor	Faint to mild
Young's modulus	4.02–4.95 GPa
Poisson ratio	0.22
Friction coefficient	0.19
Glass temperature (T_g)	50°C–55°C, uncross-linked; >200°, cross-linked
Degradation temperature (T_d)	~380°C
Boiling point	204°C
Flash point	100°C
Autoignition temperature	455°C
CTE	$52 \times 10^{-6}/\text{K}$
Thermal conductivity	0.2 W/m K
Specific heat	1500 J/kg K
Vapor pressure	0.3 mmHg at 20°C
Density (of EPON SU-8 resin)	1200 kg/m ³
Refractive index	1.668, uncross-linked; 1.67–1.8, cross-linked
Dielectric constant	4–4.5 ϵ_0
Electrical breakdown fields	~ 10^7 V/m
Resistivity	> 10^8 Ω cm

TABLE 8.2

Viscosity, Percentage of Solids, and Density of Different SU-8 Photoresist Formulations Available from MicroChem

SU-8 (Casting Solvent: Gamma-Butyrolactone)				SU-8 2000 (Casting Solvent: Cyclopentanone)				SU-8 3000 (Casting Solvent: Cyclopentanone)			
SU-8 XX	Viscosity (cSt)	% Solid	Density (g/ml)	SU-8 2XXX.X	Viscosity (cSt)	% Solid	Density (g/ml)	SU-8 30XX	Viscosity (cSt)	% Solid	Density (g/ml)
				2000.5	2.49	14.3	1.070				
2	45	39.5	1.123	2002	7.5	29	1.123				
5	290	52	1.164	2005	45	45	1.164	3005	65	50	1.075
				2007	140	52.5	1.175				
10	1050	59	1.187	2010	380	58	1.187	3010	340	60.4	1.106
				2015	1250	63.45	1.2				
25	2500	63	1.200	2025	4500	68.55	1.219	3025	4400	72.3	1.143
				2035	7000	69.95	1.227	3035	7400	74.4	1.147
50	12,250	69	1.219	2050	12,900	71.65	1.233	3050	12,000	75.5	1.153
				2075	22,000	73.45	1.236				
100	51,500	73.5	1.233	2100	45,000	75	1.237				
				2150	80,000	76.75	1.238				

density of all SU-8 photoresist formulations currently (2009) available from MicroChem and is intended to aid the reader in the process of choosing a formulation for his/her micro/nanofluidic application. The characterization of the surface properties of a material, such as electro-osmotic mobility and contact angle with aqueous-based media, is of extreme importance in microfluidics applications. It has been suggested that the SU-8 photoresist series from MicroChem possess similar electro-osmotic mobility properties to those of glass at $\text{pH} \geq 4$ (Sikanen et al., 2005). However, the authors attribute this property to the photoinitiator contained in this formulations and not to the EPON SU-8 resist itself. The surface of SU-8 is hydrophobic, with a contact angle close to 90° , but it can be rendered hydrophilic by plasma treatment or by chemical modification of the bulk (Wu et al., 2003) or the surface (Nordstrom et al., 2004).

SU-8 photoresist formulations are commercially available from MicroChem (www.microchem.com), in Newton, Massachusetts, and more recently from Gersteltec (www.gersteltec.ch), in Pully, Switzerland. The latter also offers SU-8 with different color dyes, carbon nanotubes, silica, or silver nanoparticles incorporated. MicroChem sells three different series of the product: SU-8 series, using gamma-butyrolactone (GBL) as the casting solvent, and SU-8 2000 and SU-8 3000 series where GBL is replaced by cyclopentanone. Cyclopentanone is a faster drying, more polar solvent system that results in improved coating quality and increased process throughput (Shaw et al., 2003).

Other SU-8 composition changes in the research and development stage include the use of different photoacid generators to reduce internal stress (Ruhmann et al., 2001) and the formation of copolymers with hydrophilic epoxy molecules to render the resist hydrophilic (Wu et al., 2003).

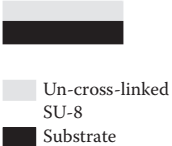
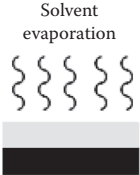
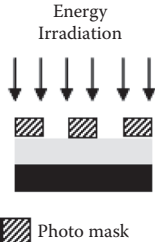
8.3 SU-8: Photolithography

Photolithography refers to the use of light to pattern a substrate. Because of, in part, its heavy use by the IC industry, UV photolithography is the most widely used form of lithography. Other resist-patterning techniques include x-ray, electron, and ion-lithography as well as soft lithography, nanoimprinting, and so forth. SU-8 photolithography generally involves a set of basic processing steps: photoresist deposition, soft bake, exposure, postexposure treatment, and developing. Descumming and postbaking might also be part of the process. A detailed resume of all the possible SU-8 photolithography steps is presented in [Table 8.3](#). When patterned at 365 nm, the wavelength at which the photoresist is the most sensitive, total absorption of the incident light in SU-8 is achieved at a depth of 2 mm. In principle, resist layers up to 2 mm thick can be structured (Bertsch et al., 1999a). Yang and Wang recently confirmed this astounding potential experimentally (Yang et al., 2005) by fabricating structures with aspect ratios more than 190 (for features with a thickness of $6 \mu\text{m}$ and a height of $1150 \mu\text{m}$). Aspect ratios greater than 10 are routinely achieved with SU-8. Aspect ratios up to 40 for lines and trenches have been demonstrated in SU-8-based contact lithography (Lorentz et al., 1998; Ling et al., 2000; Williams et al., 2004b).

For a more thorough review of the fundamentals of photolithography and its use to pattern other resists, the reader is referred to Madou (2009). The reader is also encouraged to consult other recent SU-8 reviews by del Campo et al. (2007) and Abgrall et al. (2007). [Table 8.3](#) details the process of SU-8 patterning.

TABLE 8.3

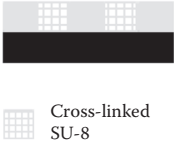
SU-8 Photolithography Processing Steps

Process Step	Process Description	Processing Parameters	Remarks
<p><i>Photoresist deposition</i></p>  <p>Un-cross-linked SU-8 Substrate</p>	<p>Photoresist is deposited on a clean substrate. Substrate materials include glass, Si, quartz, polymers, etc. Different deposition techniques exist but spin coating is the most common</p>	<p>Spin time, speed, and acceleration when using spin coating. Layer thickness is inversely proportional to spin time, speed, and acceleration</p>	<ul style="list-style-type: none"> • Layer thicknesses from a few micrometers to hundreds of micrometers (~500 μm) are possible in a single coat • Long spin times at a given speed yield better layer uniformity • Accumulation of resist on the substrate edges during spin coating causes ridges (known as edge beads), which can be removed with commercial solutions or acetone • Lamination and casting are alternatives to spin coating to deposit layers thicker than 500 μm
<p><i>Soft bake or prebake</i></p>  <p>Solvent evaporation</p>	<p>Casting solvent is evaporated from the photoresist. SU-8 does not flow at room temperature after a proper soft bake. The glass transition temperature of SU-8 resist at this point, in the uncross-linked state, is 55°C</p>	<p>Temperature and time. Soft bake temperature is usually 95°C. Times can be as short as a couple of minutes (layers <5 μm thick) or as long as hours (layers >200 μm thick)</p>	<ul style="list-style-type: none"> • The use of a hot plate is recommended to avoid <i>skin effects</i>. Baking the photoresist layer in convection ovens evaporates the solvent present on the top surface of the photoresist first, hardens the surface, and hinders the evaporation of solvent from the bulk of the photoresist • Elevated temperatures (>120°C) during soft bake can activate resist polymerization and reduce contrast • A sufficient amount of residual solvent in the soft-baked resist allows the polymer matrix to relax more and thus minimizes the residual stress, which otherwise can cause pattern debonding from the substrate at the end of the photolithography process
<p><i>Exposure</i></p>  <p>Energy Irradiation</p> <p>Photo mask</p>	<p>Irradiation from an energy source generates a low concentration of a strong acid that opens the epoxide rings of the resist and acts as a catalyst of the chemically amplified cross-linking reaction</p>	<p>Exposure dose. This value is also known as energy dose and is given by the product of the source power intensity and the exposure time. In practice, the power intensity of the source is usually fixed, and the energy dose can be varied by changing the exposure time</p>	<ul style="list-style-type: none"> • Energy sources include extreme, deep, and near-UV lights, x-rays, and ion and electron beams • SU-8 is commonly exposed using light in the near-UV range [including the i-line (365 nm) and g-line (435 nm) of a mercury lamp]. In this case, the use of a filter to eliminate light wavelengths below 360 nm is recommended to minimize <i>T-topping</i> or an exaggerated negative slope of the structure walls • SU-8 is usually exposed through a 1:1 photomask in a contact or proximity exposure setup • Multilevel topographies can be fabricated in one exposure step using GTMs or software masks • Photoresist can be exposed through the substrate (known as back-side exposure or back exposure) if the substrate has a low UV-absorption coefficient. This approach yields structure walls with shallow, positive slopes that prove ideal in molding applications

continued

TABLE 8.3 (continued)

SU-8 Photolithography Processing Steps

Process Step	Process Description	Processing Parameters	Remarks
<p><i>Postexposure bake</i></p> 	<p>The cross-linking process activated during exposure gets further activated by the application of heat. SU-8 is fully polymerized after a proper postexposure bake. The glass transition temperature of cross-linked SU-8 is more than 200°C</p>	<p>Temperature and time. More than time, PEB temperature is of crucial importance. A two-step PEB (at 65°C and 95°C for different times) is recommended by MicroChem but temperatures between 55°C and 75°C and extended baking times have been suggested to minimize internal stresses in the pattern</p>	<ul style="list-style-type: none"> • The precise control of PEB times and temperatures critically determines the quality of the final features • Insufficient PEB times and/or temperatures that are too low yield structures that are not completely cross-linked and can be attacked by the developer • Temperatures below 55°C do not polymerize the matrix completely regardless of the bake time • Thermal stresses increase with resist thickness and can cause cracking of the pattern's surface, structure bending, or complete peeling from the substrate in the worst cases • The use of a substrate material with a CTE similar to that of SU-8 can minimize thermal stresses in the pattern
<p><i>Development</i></p> 	<p>Unpolymerized SU-8 dissolves upon immersion in a developer agent such as PGMEA</p>	<p>Time and agitation rate. Development times range from few minutes (for layers thinner than 10 μm) to hours (for layers more than 400 μm thick). Agitation is usually done manually. In this case, an approximate value for the agitation rate is 60 Hz</p>	<ul style="list-style-type: none"> • Constant agitation during development is recommended to constantly feed fresh developer to the resist pattern and decrease developing times • Care must be taken when developing high-aspect-ratio structures, as excessive agitation can cause mechanical breakage • Layers thinner than 2 μm are recommended to be developed by rinsing with PGMEA instead of batch immersion in the developer • Megasonic cleaning systems can be useful to develop densely packed high-aspect-ratio structures. Megasonic frequencies are higher than ultrasonic ones and offer a less violent cavitation that prevents pattern erosion and debonding from the substrate
<p><i>Drying</i></p>	<p>This step removes the developer. Drying methods include nitrogen blowing, spinning, freeze-drying, and supercritical drying</p>	<p>Surface tension of the liquid where the SU-8 pattern is immersed before drying. The replacement of PGMEA by a liquid with lower surface tension is recommended for the prevention of structure collapse during the resist-drying process</p>	<ul style="list-style-type: none"> • Isopropyl alcohol is the most commonly used liquid to replace the developer • Stiction forces developed in narrow gaps can be strong enough to bend and join SU-8 patterns together during drying, even when using isopropyl alcohol • As the gap between high-aspect-ratio structure decreases below a few micrometers, freeze-drying and supercritical drying methods must be used

<i>Descumming</i>	A mild oxygen plasma is performed to remove unwanted resist left behind after drying. This step is not necessary for all applications and can be omitted	Oxygen pressure, polarizing voltage, and plasma exposure time. Short exposure (~1 min) of the sample to oxygen plasma created at an oxygen pressure of 200 mTorr and 200 W polarizing voltage is recommended	<ul style="list-style-type: none"> • SU-8 leaves a thin polymer film at the resist–substrate interface and on the pattern surface that is most likely due to the solid saturation of the employed developer • An alternative to oxygen plasma is a short dip immersion in acetone. SU-8 withstands acetone when fully polymerized; otherwise, the surface of the pattern will noticeably degrade • The use of a liquid phase during descumming requires a further drying step
<i>Hard bake</i>	This last bake step removes any casting solvent residue from the polymer matrix and anneals the film. This step is not necessary for all applications and can be omitted	Temperature and time. Hard baking temperatures frequently range from 120°C to 150°C. Baking times are usually longer than those used in the soft bake step	<ul style="list-style-type: none"> • Hard baking improves the hardness of the film • Improved hardness increases the resistance of the resist to subsequent etching steps • Fully cross-linked SU-8 has a glass transition temperature higher than 200°C, which makes resist reflow practically impossible
<i>Removal</i>	Removal of SU-8 from substrate. Necessary if SU-8 is used as a sacrificial material or if the substrate is to be reused	Structure thickness, amount of solvent present in the polymer matrix	<ul style="list-style-type: none"> • When using the photoresist as a sacrificial material, the primary consideration is complete removal of the photoresist without damaging the device under construction • A hard bake step is not recommended if SU-8 is intended to be removed • Dry stripping using oxygen plasma, or ashing, is recommended for a cleaner, environmentally friendly process

8.4 Resist Profiles—An Overview

Manipulation of resist profiles is one of the most important concerns of a lithography engineer. Depending on the final objective, one of the three resist profiles shown in Figure 8.2 is attempted. A reentrant, an undercut, or a reverse resist profile (resist sidewall $>90^\circ$) is required for metal lift-off. Some authors confusingly call slopes $>90^\circ$ *overcut* (Moreau, 1987); most, including these authors, refer to this type of resist profile as an *undercut*. Shallow resist angles ($<90^\circ$) enable continuous deposition of thin films over the resist sidewalls. A vertical (90° resist sidewall angle) slope is desirable when the resist is intended to act as a permanent structural element such as in microfluidics and molding applications. For more details, refer to Madou (2009). A vertical slope is desired in most microfluidics devices to avoid a flow velocity gradient (other than the one introduced by possible surface effects) along the height of the channel. Furthermore, a rectangular channel cross section is easier to model than a trapezoidal one.

8.5 Choice of Substrate

Traditionally, SU-8 photolithography is conducted on rigid substrates such as silicon, quartz, and glass. In these cases, the CTE of the substrate is significantly different from

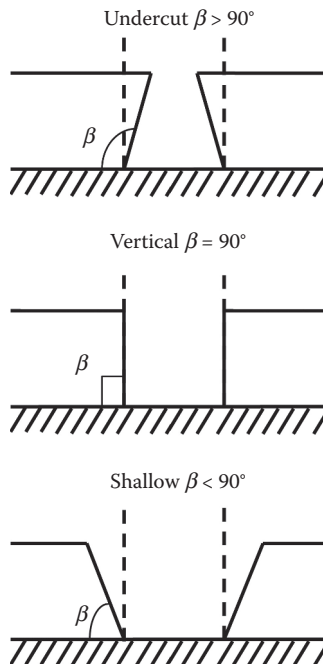


FIGURE 8.2

The three important resist profiles. A reentrant, undercut, or a reverse resist profile (resist sidewall $\beta > 90^\circ$) is required for metal liftoff. A vertical ($\beta = 75^\circ\text{--}90^\circ$ resist sidewall angle) slope is desirable for a perfect fidelity transfer of the image on the mask to the resist. Shallow resist angles ($45^\circ < \beta < 90^\circ$) enable continuous deposition of thin films over the resist sidewalls.

that of SU-8 and results in patterns with built-in stresses that may cause film cracking and distorted sidewalls. Moreover, silicon, glass, and quartz substrates are expensive and lead to a fragile, brittle microfluidics device. An inexpensive, robust material with a CTE that is close to that of SU-8 is more desirable. In Table 8.4, we list different substrate materials and their properties together with the pertinent SU-8 attributes. Polymers offer a viable option to replace silicon and glass as the substrate material. Polyetheretherketone (PEEK) and PMMA most closely resemble SU-8, with PEEK exhibiting a higher operating temperature and improved solvent resistance than PMMA (Song et al., 2004). Other viable materials from Table 8.4 include polycarbonate, polyester, and polyimide. The use of flexible film rather than rigid disk substrates allows for peeling or release of the substrate from the SU-8 patterns. Using either a 70- μm -thick PET or a 127- μm -thick polyimide film and the peeling approach, our research team obtained less-stressed freestanding SU-8 parts (Martinez-Duarte, 2009; Martinez-Duarte et al., 2009). Thick photoresist layers ($>50\ \mu\text{m}$) prove to be less brittle than thinner layers and facilitate their clean release from the film. The recommended thickness for the substrate film ranges from 50 to 130 μm . Too thin of a film tears easily and is difficult to manipulate. Films that are too thick are not as flexible and can induce sufficient stress on the structures during peeling, which causes their mechanical failure. Polymer films can be purchased in roll-to-roll sheets, and this may

TABLE 8.4

Properties of Materials Used as Substrates Compared with Those of SU-8

Material	(CTE) ($10^{-6}/\text{K}$)	Thermal Conductivity	Density (g/cm^3)	Glass Temperature or Melting Point
		at 293 K (W/m K) (Silver = 429)		
Silicon (Hull, 1999)	2.6–4.442	1.56	2.33	1414°C (1687 K)
Silicon oxide film (MEMS Exchange, 2009)	0.55	1.1	2.2	1700°C
Glass (Giancoli, 1998)	0.52	1.1	2.4–2.8	550°C–600°C
Polycarbonate (Boedeker Plastics, 2009b)	70.2	0.2	1.3	145°C
Polyimide (PI), Kapton® (Kapton Polyimide Film, 2009 and Cirlex, 2009)	20–40	0.12	1.42	360°C–410°C (633–683 K)
Polyester (PET), Mylar® (Mylar Technical Information, 2009)	17.1	0.37	1.390	254°C (527 K)
PTFE (Teflon) (FLUOROTHERM Polymers, Inc., 2009)	99	2.94	2.2	327°C
PEEK (Boedeker Plastics, 2009a)	58	0.25	1.32	249°C
PDMS (2009)	310	0.15	0.965	–125°C (uncross-linked); ~100°C (cross-linked)
PMMA (Tangram Technology Ltd., 2005)	55	0.2	1.19	65°C for standard PMMA, 100°C for heat-stabilized types
SU-8 (Chollet, 2009)	50–52	0.2	1.2	50°C–55°C (323–328 K) not cross-linked; $>200^\circ\text{C}$ ($>473\ \text{K}$) when cross-linked

open an avenue to continuous lithography of SU-8 patterns as desired (e.g., to fabricate disposable microfluidics devices for diagnostics or inexpensive molds).

Previous work on the use of polyester (Abgrall et al., 2006) or Kapton (Feng et al., 2003; Agirregabiria et al., 2005) films carrying SU-8 patterns still relied on an underling silicon or glass substrate to provide the needed rigidity for the successful application of the photoresist on these polymer films. In a novel approach, Martinez-Duarte (2009) uses aluminum support rings to hold and tighten polymer support films (drum-skin-like) to provide a rigid, planar surface ready for spin coating (see Figure 8.3). SU-8 has been patterned on both polyester and Kapton (2009) films in this manner. SU-8 processing on rigid PMMA, PTFE, PEEK, and polycarbonate disks has also been demonstrated (Song et al., 2004). For SU-8 processing on a given substrate, the chemical resistance of the substrate material to acids, bases, and solvents used in a particular SU-8 process must be investigated (e.g., when using polycarbonate and PMMA substrates, acetone should be avoided).

For many applications, the optical properties of the substrate must also be optimized. Materials with low-UV light absorption coefficient, such as glass and quartz, enable the exposure of the photoresist through the substrate, a technique referred to as back-side exposure or back exposure. Some polymers, polyester, for example, also allow for backside photopatterning. The use of back-side exposure in SU-8 photolithography yields SU-8 structures with a slight inward taper (shallow angle, $<90^\circ$) that is highly advantageous in molding and other applications. For example, thick, high-aspect-ratio SU-8 molds with positive wall slopes ($<90^\circ$) were fabricated by Martinez-Duarte (2009) using a transparent polyester film as substrate and by Peterman et al. (2003) using a Schott Borofloat® glass wafer. Kim et al. (2004) implemented backside SU-8 photolithography with a Pyrex glass substrate to fabricate tapered SU-8 pillars and later used them as templates to fabricate metallic microneedles for drug delivery. Sato et al. (2004a) and Yoon et al. (2006) combined inclined exposure (to be detailed below) and back exposure to pattern a micromesh to filter particles flowing in a microchannel. Another example is that presented by Lü et al. (2007) who used back-side exposure to fabricate SU-8 templates that were later used to electroplate nickel parts.

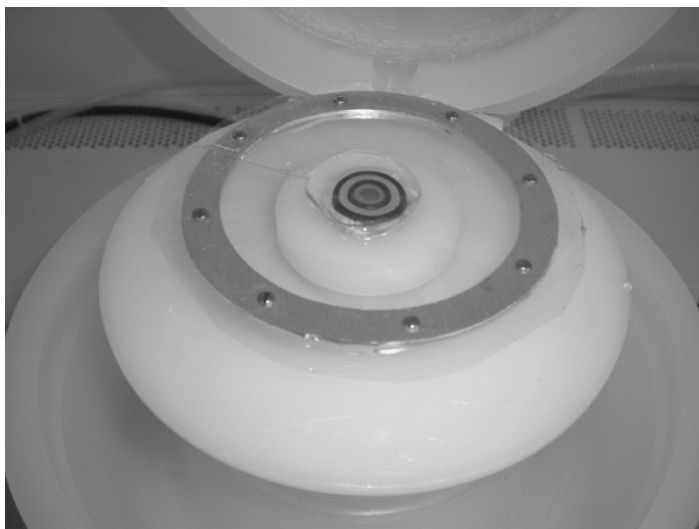


FIGURE 8.3

The use of a stretched polyester film on an aluminum ring as a substrate for SU-8 spin coating. Kapton film was also demonstrated successfully for the same purpose.

8.6 The Clean Room

To ensure industrially accepted yields, micro- and nanofabrication processes should be carried out in a *clean room*, a specially designed area where the size and the number of airborne particulates are highly controlled, together with the temperature ($\pm 0.1^\circ\text{F}$), air pressure, humidity (from 0.5% to 5% RH), vibration, and lighting (yellow to avoid resist activation). Clean rooms are classified on the basis of the number and size of particles allowed per unit volume of air. The official international standard for clean room classification is ISO 14644–1 (from the International Organization for Standardization), which specifies the decimal logarithm of the maximum number of particles 0.1 μm or larger that are permitted per cubic meter of air. For example, in an ISO 1 clean room, the particle count must not exceed ten 0.1- μm particles (or larger) per cubic meter of air, whereas in an ISO 6 clean room, the 0.1- μm particle count per cubic meter of air can be as high as one million. Although the standard FED-STD-209E, using a cubic foot as the unit volume of air (a cubic meter roughly equals 35 cubic feet), is still widely used today, it was officially cancelled by the General Services Administration of the US Department of Commerce on November 29, 2001, and was superseded by ISO 14644–1. ISO-14644 is a series of nine documents and includes additional clean room requirements that FED-STD-209E does not have, such as design and construction, operations, separation enclosures, molecular contamination, and surface contamination. Table 8.5 illustrates the different ISO classes and their FED-STD-209E equivalent.

8.7 Substrate Cleaning and Priming

Substrate cleaning is the first and a very important step in any lithographic process, as the adhesion of the resist to the substrate could be severely compromised by the presence of impurities and residual coatings. Poor adhesion can result in leaks at the substrate/SU-8 interface and compromise the performance of the microfluidic device. Contaminants

TABLE 8.5

ISO 14644–1 Clean Room Classification and FED STD 209E Equivalents

Class	Maximum Number of Particles per Cubic Meter						FED-STD-209E Equivalent
	$\geq 0.1 \mu\text{m}$	$\geq 0.2 \mu\text{m}$	$\geq 0.3 \mu\text{m}$	$\geq 0.5 \mu\text{m}$	$\geq 1 \mu\text{m}$	$\geq 5 \mu\text{m}$	
ISO 1	10	2					
ISO 2	100	24	10	4			
ISO 3	1000	237	102	35	8		Class 1
ISO 4	10,000	2370	1020	352	83		Class 10
ISO 5	100,000	23,700	10,200	3520	832	29	Class 100
ISO 6	1,000,000	237,700	102,000	35,200	8320	293	Class 1000
ISO 7				352,000	83,200	2930	Class 10,000
ISO 8				3,520,000	832,000	29,300	Class 100,000
ISO 9				35,200,000	8,320,000	293,000	Room air

TABLE 8.6

Some Common Clean Room Contaminant Sources

Location: a clean room near a refinery, smoke stack, sewage plant, and cement plant spells big trouble
Construction: the floor is an important source of contamination. Also, items such as light fixtures must be sealed, and room construction tolerances must be held very tight
Wafer handling: transfer box
Process equipment: never use fiber glass duct liner; always use 100% polyester filters, and eliminate all nonessential equipment
Chemicals: residual photoresist or organic coatings, metal corrosion
Attire: only proper attire and dressing in the anteroom
Electrostatic charge: clean room must have a conductive floor
Furniture: only clean room furniture
Stationary: use ballpoint pen instead of lead pencil; use only approved clean room paper
Operator: no eating, drinking, smoking, chewing gum, or makeup of any kind

include solvent stains (methyl alcohol, acetone, trichloroethylene, isopropyl alcohol, xylene, etc.) and airborne dust particles from operators, equipment, smoke, and so forth (see Table 8.6). As previously noted, SU-8 photolithography makes use of different kinds of substrates, and thus a cleaning procedure must be chosen accordingly. Wet immersion cleaning carried out using diluted hydrofluoric acid, Piranha (a mix of sulfuric acid and hydrogen peroxide at different ratios including 5:1 and 3:1. Note that this mixture is exothermic. When cool, it may be refreshed by very slowly adding more hydrogen peroxide), and RCA (a process developed by W. Kern that involves ammonium hydroxide, hydrogen peroxide, DI water, and hydrofluoric and hydrochloric acids at different stages*) can only be used with silicon or glass substrates. Milder, but not as effective, procedures such as DI water rinsing followed by solvent rinse can be used for the cleaning of certain polymer substrates. Other cleaning methods for substrates include ultrasonic agitation, polishing with abrasive compounds, and supercritical cleaning in which the liquid-solvative properties, gas-like diffusion, and viscosity of critical fluids, CO₂, for example, enable rapid penetration into crevices for a complete removal of organic and inorganic contaminants contained therein (McHardy et al., 1998; King et al., 2003). Gaseous cleaning methods include vapor cleaning, thermal treatment, (e.g., baking the substrate at 1000°C in vacuum or in oxygen), and plasma or glow discharge techniques (e.g., in Freon® with or without oxygen). In general, vapor phase cleaning methods use significantly less chemicals than wet immersion cleaning and because the US Environmental Protection Agency regulations are becoming the preferred methods. In the case of wet immersion cleaning, dehydration before resist deposition is recommended as humidity plays a crucial role in the adhesion of SU-8 to the substrate.

Poor adhesion of SU-8 photoresist to a given substrate is also due to partial wetting of the substrate surface and can occur even if a clean substrate is used. Modification of the substrate surface chemistry can significantly improve the adhesion of a photoresist to a substrate. Common adhesion promoters such as hexamethyldisilazane, AP300, and methacryloxy [propyl] trimethoxysilane, effectively prime the substrate surface for photoresist deposition. MicroChem's Omni-coat and Gersteltec's adhesion promoter are two choices optimized to improve SU-8 adhesion to the substrate. Adhesion promoters are not

* The prevalent RCA1 and RCA2 wet cleaning procedures are as follows: RCA1: add one part of NH₃ (25% aqueous solution) to five parts of DI water and heat to boiling and add one part of H₂O₂. Immerse the substrate for 10 min. This procedure removes organic dirt (resist). RCA2: add one part of HCl to six parts of DI water and heat to boiling and add one part of H₂O₂. Immerse the substrate for 10 min. This procedure removes metal ions.

always necessary, and the reader, to save cost and time, is encouraged to pattern SU-8 on the bare substrate first and characterize the results. SU-8 exhibits good adhesion to Si and Si/SiO₂ but poor adhesion to glass substrates. From the metals commonly used in microfabrication, Al offers the strongest adhesion for SU-8 followed by Ti and Au. The quality of adhesion of SU-8 to Cu and Cr has been reported to depend inversely on feature size, with smaller features exhibiting the best performance. From the metals investigated, Ni exhibits the lowest adhesion strength (Dai et al., 2005; Nordström et al., 2005; Barber et al., 2007). The choice of the casting solvent in a photoresist composition is also important. For example, the use of cyclopentanone instead of gamma butyrolactone produces a photoresist composition with lower surface tension that improves SU-8 spreading characteristics (Shaw et al., 2003).

8.8 Photoresist Deposition

Spin coating is the current method of choice to deposit SU-8 photoresist. A uniform layer ranging in thickness from a few to hundreds of micrometers can be deposited by simply tuning spin profile parameters such as time, speed, and acceleration and using an appropriate SU-8 photoresist formulation (thicker layers benefit from more viscous formulations). Successive spin coating and baking steps of individual SU-8 layers lead to a total thickness of up to 2 mm. Spin coating features three steps: dispensing, spreading, and coating. In the first step, the photoresist is dispensed onto a substrate held in place by a vacuum-actuated chuck in a resist spinner (Metz et al., 1992). Dispensing too much resist onto the substrate results in edge covering or run-out; too little resist may leave uncovered areas. The resist must be dispensed at the center of rotation of the substrate. Dispensing resist on an area other than the center of rotation leads to an imbalance on the centripetal forces acting on the resist puddle during spinning that causes nonuniform coatings. The shape of the substrate must also be taken into account to guarantee a uniform coating. Circular substrates benefit from dispensing in one single spot such that the resist puddle takes in a circular shape after dispensing. Rectangular substrates benefit instead from dispensing in several continuous spots (think of a line). A time after dispensing and before spreading is recommended for the photoresist to relax and eliminate air bubbles introduced during dispensing. Low rotation speeds (<100 rpm) during resist dispensing may also prove beneficial. The second step, spreading, uses a rotating speed of approximately 500 rpm for 10–20 s to spread the fluid over the substrate. Acceleration for this step is recommended to be approximately 100 rpm/s. After spreading the photoresist, higher rotating speeds are used to thin down the fluid near to its final desired thickness and completely coat the substrate. Typical values for this step include spin speeds in the range of 1000 to 4000 rpm, spin acceleration between 200 and 500 rpm/s, and spinning times from a few seconds to several minutes. The reader is referred to either MicroChem's or Gersteltec's processing data sheets for guidelines on how to optimize spin parameters and obtain a specific layer thickness, given a photoresist formulation. In general, the last number(s) of the resist formulation name (see [Table 8.2](#)) depicts the layer thickness that is obtained when spinning at 3000 rpm for 30 s. For example, the spin coating of MicroChem's SU-8 2010 at 3000 rpm for 30 s yields a 10- μ m-thick layer; the use of SU-8 100 under the same parameters yields a 100- μ m-thick layer. Layer uniformity is improved by using prolonged spin times (Chen et al., 2001), but this decreases the layer thickness. The final layer thickness is inversely

proportional to spin speed, acceleration, and time but directly proportional to solution concentration and molecular weight (measured by intrinsic viscosity) of the photoresist. Inherent to spin coating is the formation of edge beads or photoresist ridges that can be approximately 10 times higher than the mean thickness of the rest of the substrate. This introduces air gaps between the mask and the surface of the photoresist that can lead to pattern broadening because of light diffraction and nonuniform exposure throughout the substrate. For SU-8 formulations with low viscosity (<7000 cSt), the edge bead is likely to disappear because of reflow of the photoresist after spin coating. For thicker formulations, commercial edge bead removal solutions such as MicroChem's edge bead removal solution can be used. Other alternatives include GBL and acetone. Edge bead removal is commonly integrated in the spin-coating process and is carried out immediately after the coating of the photoresist layer.

An empirical expression to predict the thickness of the spin-coated film as a function of its molecular weight and solution concentration has been given by Thompson (Thompson, 1994). For theoretical analysis and modeling of the rheology of the spin-coating process, the reader is referred to the works of Schwartz et al. (2004), Acrivos et al. (1960), Emslie et al. (1959), and Washo (1977).

Optimization of the photoresist coating process in terms of resist dispense rate, dispense volume, and spin speed presents a growing challenge. SU-8 photoresists currently average US\$ 1000 per liter (2009) and make processing optimization necessary. The need for an alternative photoresist deposition technique arises as the amount of waste material generated by spin coating is high, with most of the resist solution (>95%) thrown off the substrate during the spin casting process (the waste resist must be disposed as a toxic material). For example, in spray coating, the substrates to be coated pass under a spray of photoresist solution. The spray system includes an ultrasonic spray nozzle that generates a distribution of droplets in the micrometer range.

Spray coating does not suffer from resist thickness variation caused by the centrifugal force because the resist droplets are supposed to stay where they are being deposited. Because of the same reason, the amount of photoresist wasted during spray coating is significantly less than that with spin coating. In a spray coating system, the resist is pushed out of a pressurized tank via a supply pipe to the spray head that has a defined aperture where the spray mist is formed. The shape of the spray pattern can be adjusted by a secondary air cushion, and undesired overspray can be minimized by keeping the spray gun close to the substrate (~5 cm). A major advantage of this technique is its ability to coat uniformly over nonuniform surfaces, making the technique appropriate for substrates with three-dimensional topographies such as those used in MEMS and microfluidics. Importantly, sprayed coatings do not have the internal stress forces that are common in spin-coated films. The process can be automated and may coat substrates double-sided. The disadvantages of spray coating include its inability to control the thickness of the deposited film as precisely as spin coating and that it is difficult to deposit layers thicker than 20 μm .

Other photoresist deposition methods include electrostatic spraying, a variant of spray coating, and roller, curtain, extrusion, dip, and meniscus coating. As with spray coating, these techniques are not as efficient when depositing layers thicker than tens of micrometers. Alternatives for the deposition of thick layers include casting (Lin et al., 2002), silk-screen printing, and lamination (Abgrall et al., 2008). Unfortunately, SU-8 dry laminated sheets are not commercially available yet and must be fabricated in-house. For more details on alternative techniques to spin coating for photoresist deposition, the reader is referred to Madou (2009).

8.9 Soft Baking or Prebaking

After coating, the photoresist still contains 4–24 wt% solvent, depending on the thickness of the layer. Layers thinner than 20 μm contain less than 10% solvent, whereas thicker layers, 100 μm or greater, can contain up to 24% solvent. The photoresist must be soft baked (also known as preexposure bake or prebake) for a given time in an oven or on a hot plate at temperatures ranging from 65°C to 100°C (Feng et al., 2003; Anhoj et al., 2006) to remove solvents and stress and to promote adhesion of the resist layer to the substrate. SU-8 soft bake is usually conducted at 95°C. Hot-plating the resist is faster, more controllable, and does not trap solvent as convection oven baking does. In convection ovens, the solvent at the top surface of the resist is evaporated first, and this can cause an impermeable resist skin, trapping the remaining solvent inside. Soft bake was considered a trivial step in the SU-8 photolithography process until Zhang et al. (2001) demonstrated a substantial increase in patterning resolution and overall device yield. Excessive or extended baking leads to a decrease in material hardness and an increase in crack density. The presence of cracks in the SU-8 surface introduces crevices that can distort the flow field or act as random physical traps for cells, DNA, and other objects of interest. Elevated soft bake temperatures (>120°C) result in thermal activation of the photoinitiator and reduced contrast, leading to line broadening and poor resolution. It has been suggested that the presence of a certain amount of solvent in the resist after the prebake increases the effective concentration of the polymerization catalyst during exposure, leading to improved sensitivity and yielding a better cross-linked (stronger) material (Anhoj et al., 2006). A sufficient amount of residual solvent in the soft-baked resist also allows the polymer matrix to relax more and thus minimizes the residual stress that otherwise can cause delamination of the final resist structures. However, excessive solvent in the polymer matrix can lead to bubbles and cause a stress gradient to form during postexposure baking. Solvent pockets in the final SU-8 structure create weak points in the matrix that compromise the mechanical integrity of the pattern (more details are presented below under hard bake).

The rate of solvent loss is determined by the solvent diffusion coefficient. This number increases with temperature and has been suggested to decrease exponentially with the amount of solvent present in the polymer–solvent system (Vrentas et al., 1977a, 1977b). Experimental data suggest that the bulk of the solvent contained in the photoresist evaporates within the first 5 min of the bake (Shaw et al., 2003). Because the amount of solvent in the resist exponentially decreases with baking time, the solvent evaporation rate also reduces exponentially as soft bake time increases. The difference in the evaporation rates of different solvents, for example, between gamma-butyrolactone and cyclopentanone, tends to disappear as the thickness of the layer increases (Shaw et al., 2003). Thick resists may benefit from a longer bake time to completely remove the solvent.

The resist must be allowed a period of relaxation after the soft bake and before exposure for the resist and substrate to cool down to room temperature. A disagreement on the optimal relaxation time exists; some authors suggest relaxation times of hours (e.g., Anhoj et al., 2006), whereas others, including the current authors, suggest a few minutes (<5 min) [e.g., Williams et al. (2004b) and our own team’s practice—not published].

8.10 Exposure

After soft baking, the resist-coated substrates are transferred to an illumination or exposure system where they are aligned with the features on a photomask. For any lithographic technique to be of value, it must provide a very precise alignment technique capable of aligning the mask and substrate within a small fraction of the minimum feature size of the devices under construction. In the case of SU-8 photolithography, exposure is normally conducted in contact or proximity systems that consist of a UV lamp illuminating the resist-coated substrate through a mask without any lenses between the two.* The purpose of the illumination systems is to deliver light with the proper intensity, directionality, spectral characteristics, and uniformity across the substrate, allowing a nearly perfect transfer or printing of the mask image onto the resist in the form of a latent image. The incident light intensity (in W/cm^2) multiplied by the exposure time (in seconds) gives the incident energy (J/cm^2) or dose, D , across the surface of the resist film. Radiation induces the generation of a strong acid that initiates polymerization in the exposed areas. The smaller the dose needed to transfer the mask features onto the resist layer with good resolution, the better the sensitivity. Pattern geometry, including area and thickness, has a strong influence on the required dose. Large-area thick patterns, commonly required in microfluidics, require a higher exposure dose than small-area shallow patterns.

The absolute minimum feature size in a miniature device, whether it involves a channel width, spacing between features, or contact dimension, is called the *critical dimension*. A critical dimension defines the overall resolution of a process, that is, the consistent ability to print a minimum size image, under conditions of reasonable manufacturing variation (Wolf and Tauber, 2000). Many aspects of the process, including hardware, photoresist, and processing considerations, can limit the resolution of photolithography. Hardware limitations that include diffraction and reflection of light (or scattering of charged particles in the case of charged-particle lithography or hard x-rays), lens aberrations, and mechanical stability of the system (vibrations) must all be minimized. The resist material properties that impact resolution include sensitivity, contrast, and energy absorption at different wavelengths.

Light wavelengths used in SU-8 photolithography range from the very short of extreme UV (10–14 nm) to deep UV (150–300 nm) to near UV (350–500 nm). Other energy sources amenable to induce SU-8 cross-linking have shorter wavelengths yet and include x-ray (0.01–10 nm) and electron (0.12 nm to 7 pm in the energy range 100 eV to 30 keV) and ion (2.8–0.16 pm also in the energy range 100 eV to 30 keV) beams. X-ray techniques enable the fabrication of SU-8 structures with very high aspect ratios (Bogdanov et al., 2000; Shew et al., 2004; Barber et al., 2005; Tan et al., 2006; Reznikova et al., 2008), whereas nanometer-sized features have been fabricated with EBL and ion-beam lithography[†] (van Kan et al., 1999; Aktary et al., 2003; Nallani et al., 2003; Pépin et al., 2004; Bilenberg et al., 2006; Robinson et al., 2006). It was shown that SU-8 is more sensitive to x-ray and electron beams than PMMA, the traditional material of choice.

Here, we focus on SU-8 patterning with light wavelengths in the near-UV range where one typically uses the g-line (435 nm) or i-line (365 nm) of a broadband mercury lamp. SU-8 photoresists feature a high absorption of energy of wavelengths that are less than 350 nm. One of the main reasons for this is that triarylsulfonium hexafluoroantimonate

* In contrast to projection lithography where the pattern is imaged onto the resist through a lens.

† Ion beams undergo less scattering than electron beams and achieve higher resolution.

salt, used as photoacid generator in common SU-8 photoresist formulations, has absorption bands at 231.5, 268.5, and 276 nm, as measured in methanol solution (Crivello et al., 1979). When SU-8 is exposed using a broadband mercury lamp, UV light shorter than 350 nm is strongly absorbed at the photoresist's top surface. This causes the creation of more acid that diffuses sideways and polymerizes a thin layer along the top surface of the resist film. This effect is commonly known as *T-topping* and is illustrated in Figure 8.4. Selective filtration of the light from the light source is required to eliminate the undesirable shorter wavelengths and to obtain a vertical wall that is desired in most microchannels. An easy and affordable way to implement a filter is by using a 50- to 100- μm layer of SU-8 placed in between the light source and the mask. Commercial high-pass filters with a cutout wavelength of 360 nm are also available. For example, Reznikova et al. (2005) used a 100- μm -thick SU-8 resist layer to filter exposure radiation at 334 nm, and Lee et al. (2003) reported using a commercial Hoya UV-34 filter to eliminate the T-topping.

Introduction of a filter between the photoresist surface and the light source attenuates the incident light intensity at the SU-8 film. It is necessary to take this attenuation factor, and any others introduced by elements in the optical pathway between the light source and the photoresist (Figure 8.5), into account and adjust the exposure dose accordingly. The following relation must be obeyed:

$$\text{Experimental dose} = \frac{\text{Recommended dose}}{t_1 \times t_2 \times t_3 \times \cdots \times t_n} \quad (8.1)$$

where t denotes UV transmission percentage of an element n in the optical pathway. The recommended dose is the value recommended in the SU-8 processing data sheets, whereas the experimental dose is the one implemented in practice. Underexposure causes the intended pattern to dissolve or to lift off during developing because the cross-linking acid concentration was not enough to fully polymerize the resist all the way to the underlying substrate. Overexposure leads to extreme T-topping and pattern broadening.

Besides T-topping, the Fresnel diffraction is also responsible for the decrease in resolution and pattern broadening at the resist-air interface of the structure (Chuang et al., 2002; Yang et al., 2005). SU-8 exposure is commonly carried out in a contact or proximity mode. In contact mode, the resist-coated substrate is brought into contact with the mask (Figure 8.5), whereas in proximity mode, the resist's top surface is 10–20 μm away from the mask.

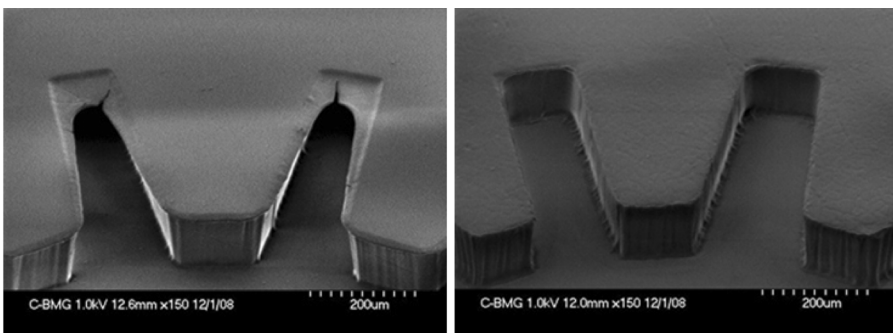
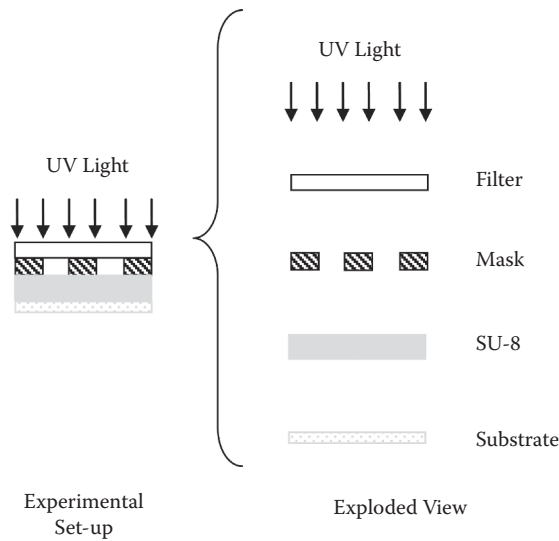


FIGURE 8.4

The effect of T-topping. Left: gear pattern showing T-topping. Right: same gear pattern but now T-topping is minimized by the use of an in-house fabricated filter (a 50 μm layer of SU-8 on glass).

**FIGURE 8.5**

Optical pathway between light source and SU-8 surface in a common exposure setup.

The contact mode can be further classified as soft contact and hard contact depending on the amount of contact pressure between the resist and the mask, with higher pressures being applied in hard contact mode. Exposure in a contact or proximity setup results in a 1:1 image of the entire mask onto the photoresist. The three setups introduce air gaps, with hard contact minimizing the size of such gaps, between the mask and the resist surface that amplify light diffraction and cause pattern broadening because of the difference between the refractive indexes of air and SU-8. These gaps are often the result of an edge bead or the use of an accidentally inclined hot plate. Different measures can minimize the negative impact of air gaps. For example, the air gaps were filled with glycerol (refractive index $n = 1.473$) by Chuang et al. (2002), whereas Yang et al. (2005) used a type of refractive-index-matching liquids from Cargille Laboratories, in Cedar Grove, New Jersey, to exactly match the refractive index of SU-8 ($n = 1.668$). The use of the latter matching liquid allowed for the fabrication of structures with aspect ratio greater than 190:1. The reflection of light on certain substrates also degrades wall verticality, broadens the pattern, and adds another parameter to consider when setting the exposure time and intensity (Zhang et al., 2004).

8.11 Masks and Gray Scale Lithography

The stencil used to repeatedly generate a desired pattern on resist-coated substrates is called a mask. Like resists, masks can be positive or negative. A positive or a dark-field mask is a mask on which the pattern is clear with the background dark. A negative or a clear-field mask is a mask on which the pattern is dark with the background clear. SU-8 microfluidic devices are usually fabricated with negative or clear-field masks where the microchannels, reservoirs, sample inlets, and so forth, are denoted by dark patterns on

a clear background. A light-field or a dark-field image, known as mask polarity, is then transferred to the surface. Masks can be further classified using a criteria similar to that described above for exposure setups. Masks that make direct physical contact with the substrate are called contact masks and degrade faster than noncontact, proximity masks, which are slightly raised, say 10–20 μm , above the substrate. However, diffraction effects are minimized by the use of contact masks. Contact masks are classified as hard contact and soft contact masks. In both cases, one brings the resist-coated wafer into contact with a mask, but by using more pressure, in a hard contact mask setup, the gap between the wafer and the mask can be further reduced. Contact masks, mainly the soft contact type, are still in use in research and development, in mask making itself, and in prototyping. Contact mask and proximity mask printing are collectively known as shadow printing. A more reliable method of masking, but significantly more expensive, is projection printing where, rather than placing a mask in direct contact with (or in proximity to) a substrate, the photomask is imaged by a high-resolution lens system onto the resist-coated substrate. In projection printing, the only limit to the mask's lifetime results from operator handling. Mask fabrication is less challenging in projection lithography because the imaging lens can reduce the mask pattern by 10:1, although reduction values of practical systems are 4:1 or 5:1 (Levinson, 2005). Diffraction can be minimized by the use of highly collimated light sources and/or collimator lenses. Projection lithography is the printing method used in the fabrication of devices based on very large scale integration, such as ICs.

In miniaturization science, one is often looking for low-cost and fast-turnaround methods to fabricate masks. Besides the traditional photomask—a nearly optically flat glass (transparent to near UV) or quartz plate (transparent to deep UV) with an absorber pattern metal layer (e.g., an 800-Å-thick chromium layer) generated by EBL—other less expensive approaches are common. These may involve in-house fabricated masks by manually drawing patterns on cut-and-peel masking films and photoreducing them. Alternatively, these may involve direct writing on a photoresist-coated plate with a laser-plotter (~2- μm resolution) (Arnone, 1992). Simpler yet, using a drawing program such as Canvas™ (ACD Systems, Ltd.), Freehand®, Illustrator® (Adobe Systems, Inc.), or L-Edit™ (Tanner Research, Inc.), a mask design can be created on a computer and saved as a PostScript® or Gerber file to be printed with a high-resolution printer on a transparent film (Duffy et al., 1998a). The transparency with the printed image may then be clamped between a presensitized chrome-covered mask plate and a blank plate to make a traditional photomask from it. After exposure and development, the exposed plate is put in a chrome etch for a few minutes to generate the desired metal pattern, and the remaining resist is stripped off. Simpler yet, the printed transparency may be attached to a blank quartz plate and used directly as a photolithography mask. The maximum resolution with transparency methods is currently around 7 μm (2009) and is highly dependent on the photoplotter used to print the transparency. Although transparency masks are significantly less expensive and have a fast-turnaround time, the quality of the exposed patterns, that is, wall roughness, and the resolution are obviously less than those obtained with photomasks patterned with EBL (where the resolution can be as high as 10 nm) (see [Figure 8.6](#)).

Photolithography, as described so far, constitutes a binary image transfer process—the developed pattern consists of regions with resist (1) and regions without resist (0). In contrast, in gray scale lithography, the partial exposure of a photoresist renders it soluble to a developer in proportion to the local exposure dose, and as a consequence, after development, the resist exhibits a surface relief or three-dimensional topography. This way, covered microchannels and complex fluid networks can be fabricated in a single exposure step to eliminate further bonding of a separate top cover needed to close a channel fabricated

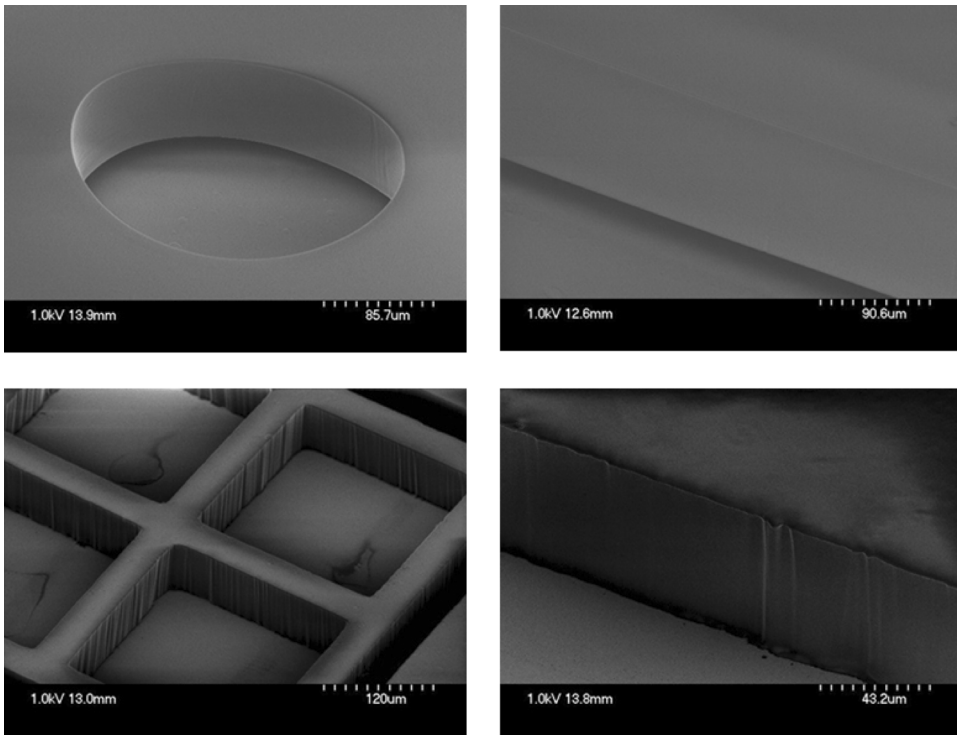


FIGURE 8.6

The quality of a pattern is far superior when using photomasks patterned with EBL (top) than when using transparency masks printed with a commercial photo-plotter (bottom).

with conventional SU-8 photolithography. Gray scale lithography has a great potential use in miniaturization science as it allows for the mass production of microstructures with varying topography. The possibility of creating profiled three-dimensional microstructures offers tremendous additional flexibility in the design of microfluidic, micro-electronic, optoelectronic, and micromechanical components (Sure et al., 2003). A key part in the development of a gray scale process is the characterization of the resist thickness as a function of the optical density in the mask for a given lithographic process. It is also desirable to use photoresists that exhibit a low contrast to achieve a wide process window. Ideally, the resist response can be linearized to the optical density within the mask. Gray scale lithography can be achieved using gray-tone masks (GTMs) and software masks. Possible methods for making GTMs, or variable transmission masks, include magnetron sputtering of amorphous carbon onto a quartz substrate. Essentially any transmittance (T) desired in the $0\% < T < 100\%$ range can be achieved by controlling the film thickness (t) in the $200\text{-nm} > t > 0\text{-nm}$ range with subnanometer precision (Windt et al., 1999). Perhaps more elegantly, gray levels may be created by the density of dots that will appear as transparent holes in a chromium mask. These dots must be small enough not to be transferred onto the wafer because they are below the resolution limit of the exposure tool; otherwise, pixelation might occur. Another attractive way to fabricate a GTM is with high-energy beam-sensitive (HEBS) glass. HEBS glass turns dark upon exposure to an electron beam; the higher the electron dosage, the darker the glass turns. In HEBS glass, a top layer, a couple of microns thick, contains silver ions in the form of silver-alkali-halide

(AgX)_m (MX)_n complex nanocrystallites that are approximately 10 nm or less in size and are dispersed within cavities of the glass SiO₄ tetrahedron network. Chemical reduction of the silver ions produces opaque specks of silver atoms upon exposure to a high-energy electron beam (>10 kV) (Sure et al., 2003). Another example of a GTM was demonstrated by Hung et al. (2005). A positive resist is first patterned on a glass substrate and reflowed to obtain curved structures. These curved extrusions are then used as a GTM mask to fabricate cups in SU-8 using glycerol to fill the air gap between the GTM and the SU-8 surface. The use of microfluidics in GTM technology was demonstrated by Chen et al. (2003) using PDMS microchannels as photomasks. The microchannels are filled and emptied at will with light-absorbing liquids, that is dyes, to enable rapid reconfiguration to different gray scale patterns. The authors claim an unlimited number of gray scales given by variations in dye concentration and composition. A similar approach but without the use of microfluidics is the use of colored masks as demonstrated by Taff et al. (2006), where they first characterized the UV absorption of different colors, printed on a transparent film using a standard laser color printer, and then fabricated SU-8 holes of varying depths depending on the color used during exposure.

An alternative to GTMs is the use of maskless optical projection lithography techniques, where a physical mask is replaced by a *software mask*. One approach to make multilevel photoresist patterns directly with a software mask is by variable-dose electron beam writing, in which the electron dosage (the current multiplied by the dwell time) is varied across the resist surface (Stauffer et al., 1992). A laser writer can produce a similar topography but at a lower resolution (Yu et al., 2006). However, variable-dose electron beam and laser writing are serial, slow, and costly, making GTMs a better alternative if high-throughput production is required. A gray scale lithography technique that uses a software mask and yet allows for batch fabrication is based on the digital micromirror device (DMD) chip from Texas Instruments, Inc. and relies on the same spatial and temporal light modulation technology used in digital light processing projectors and high-definition televisions. A commercial instrument based on this chip is offered by Intelligent Micro Patterning LLC. Enormous simplification of lithography hardware is feasible by using the movable mirror arrays in a DMD chip to project images on the photoresist. This technique is capable of fabricating micromachined elements with any surface topography and can, just like EBL or laser writing, be used for implementing maskless binary and gray scale lithography. The maximum resolution of DMD-based maskless photolithography (1 μm in 2009) is far less than with EBL (~10 nm) or laser writers (<1.0 μm), but it is a parallel technique, and for many applications, microfluidics, for example, the lower resolution might not be an obstacle. Unfortunately, the maximum field of exposure is currently (2009) only a few square centimeters, and image stitching is necessary if a large-area pattern is to be fabricated. The unique capability of representing a gray scale is probably the most essential merit of this type of maskless lithography. When a mirror is switched on more frequently than switched off, it reflects a light gray pixel; a mirror that is switched off more frequently reflects a darker gray pixel. In this way, the mirrors in a DMD system can reflect pixels in up to 1024 shades of gray to convert the video or graphic signal entering the DMD chip into a highly detailed gray scale image. Examples of gray scale features obtained with this type of maskless lithography are shown in [Figure 8.7](#).

Another interesting technique to fabricate gray scale structures includes the tilting and/or rotation of the substrate stage with respect to the UV source (Beuret et al., 1994; Han et al., 2004; Yoon et al., 2006) to fabricate pillars, V-grooves, cones, and other structures as illustrated in [Figure 8.8a](#). One of the most astonishing applications is the fabrication of three-dimensional gratings embedded in a microchannel, as shown in [Figure 8.8b](#)

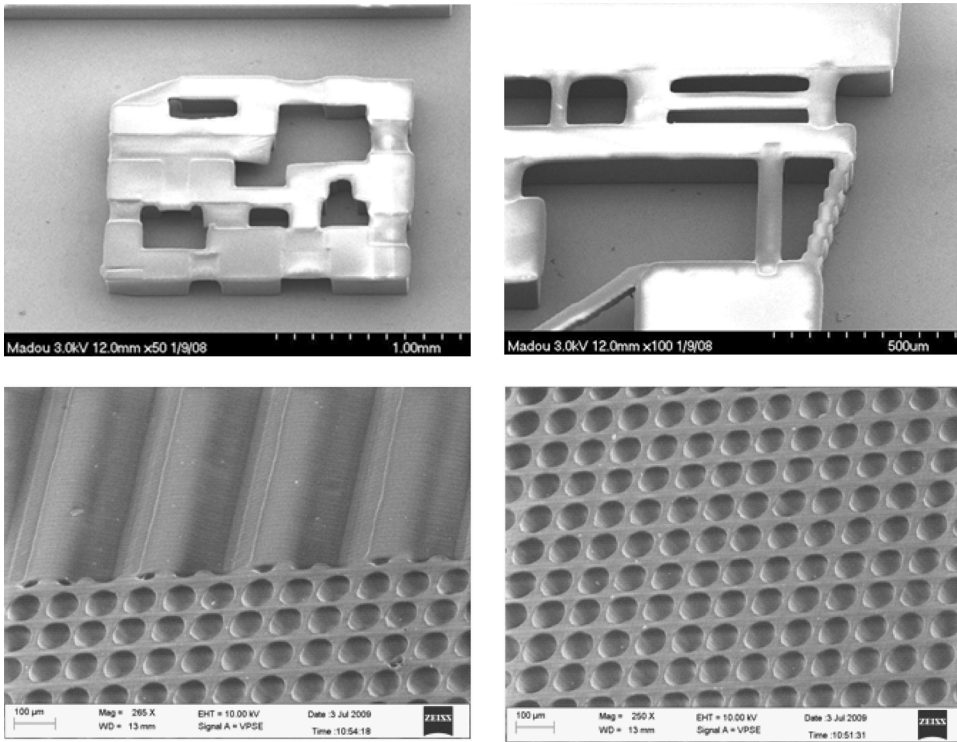


FIGURE 8.7

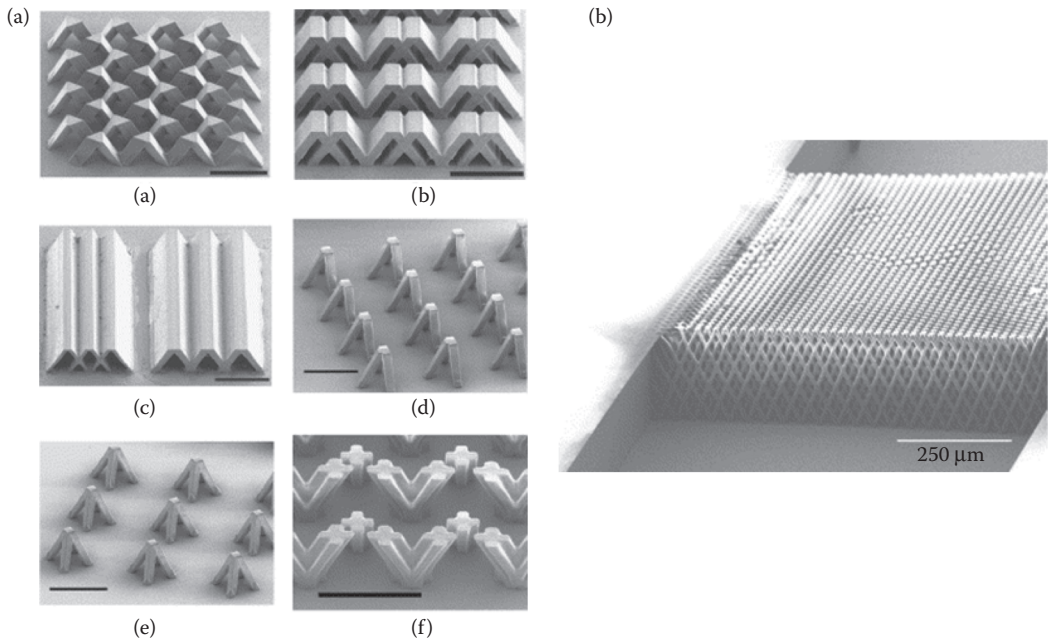
Examples of gray scale lithography obtained with an SF-100 maskless lithography system (Intelligent Micro Patterning, LLC) using SU-8 photoresist. (Courtesy of P. Dwivedi and A. Sharma at the Indian Institute of Technology in Kanpur, India. With permission.)

(Sato et al., 2004b). The combination of tilting and rotation is also capable of fabricating embedded channels in a single exposure step. The angle of the structure depends on both the inclination of the holding stage and the refractive indexes of the different materials in the optical path between the light and the photoresist. The elimination of air gaps is also desired in this setup to improve the maximum tilt angle of the structures (Hung et al., 2004).

Other gray scale exposure techniques include moving mask lithography (Hirai et al., 2007), holography (Deubel et al., 2004; Ullal et al., 2004), and stereolithography (Bertsch et al., 1999b).

8.12 Postexposure Bake

In the case of a chemically amplified resist, such as SU-8, the postexposure bake (PEB) is critical to complete the cross-linking of the polymer matrix. Although reactions induced by the catalyst formed during exposure take place at room temperature, their rate is significantly increased by baking at 60°C–100°C. The precise control of PEB times and temperatures critically determines the quality of the final features and the performance of the pattern as a mold or as a structural element for microfluidics. More than time, PEB temperature

**FIGURE 8.8**

(a) Different geometries obtained with inclined exposure. (Reprinted from *Sensors and Actuators A Physical* 111, Han, M., W. Lee, S. Lee, and S. S. Lee, 3D microfabrication with inclined/rotated UV lithography, 14–20, Copyright (2004), with permission from Elsevier.) (b) A grating embedded in a microchannel. (Reprinted from *Sensors and Actuators A: Physical* 111(1), Sato, H., T. Kakinuma, J. S. Go, and S. Shoji, In-channel 3-D micromesh structures using maskless multi-angle exposures and their microfilter application, 87–93, Copyright (2004a), with permission from Elsevier.)

is of crucial importance; longer times at lower temperatures are recommended. High PEB temperatures have been shown to induce a high amount of internal stress in the structure when using traditional substrates such as silicon and glass. The reason behind this is the significant difference between the coefficients of thermal expansion (CTE) of SU-8 and the substrate as discussed previously. Thermal stresses increase with resist thickness and can cause cracking of the pattern's surface, structure bending, or complete peeling from the substrate in the worst cases. These defects are most likely to be present in extended, large surface area features as the ones required in microfluidics and in those with sharp angles and can be minimized by choosing an alternative substrate, a polymer, one for example, or by reducing the pattern dimensions, if the application allows it. On the other hand, insufficient PEB times and/or temperatures that are too low yield structures that are not completely cross-linked and that can be attacked by the developer. This causes extremely high surface roughness or even complete dissolution of the photoresist. MicroChem's processing data sheets (MicroChem Corp.) recommend PEB to be carried out at 95°C, but temperatures between 55°C and 75°C and extended baking times have been suggested to minimize internal stresses in the pattern. Temperatures below 55°C do not polymerize the matrix completely regardless of the bake time (Li et al., 2005). Rapid heating and cooling of the resist should be avoided as swift temperature changes induce a significant amount of stress. Controlled cooling and heating rates are suggested, and the slower the temperature ramps, the better the results (Williams et al., 2004b). The current authors believe that the use of a convection oven benefits the PEB step as thermal energy is applied more uniformly across

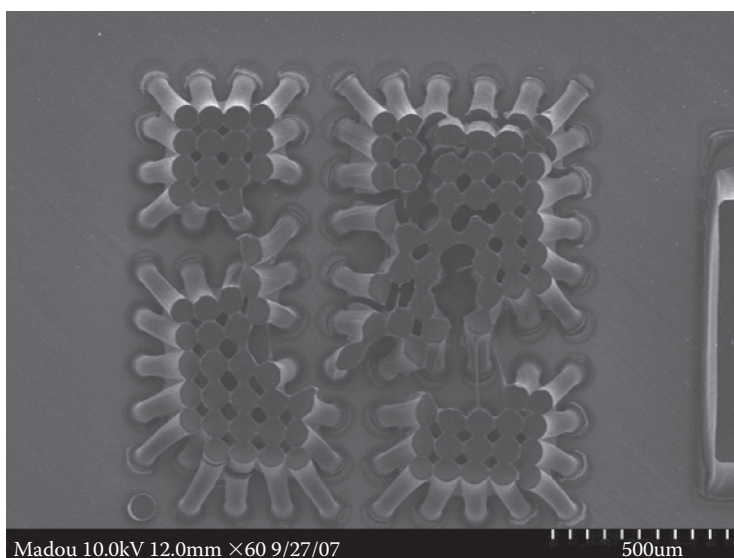
the surface of the polymer structure, but no studies have been performed to confirm this point. The replacement of silicon and glass substrates by those having a CTE similar to that of SU-8, for example, polymers, can prove to be very beneficial.

SU-8 microfluidic devices benefit from an optimal PEB to improve adhesion, reduce scumming (resist left behind after development), increase contrast and resist profile (higher edge-wall angle), and reduce the effects of standing waves in an SU-8 resist.

8.13 Development

Development is the dissolution of unpolymerized SU-8 that transforms the latent resist image, formed during exposure, into a relief topography that can serve as a mold or as a permanent structural element. In general, two main technologies are available for resist development: wet development and dry development. The latter is starting to replace wet development for some of the ultimate line-width resolution applications, but wet development is still widely used in a variety of applications, including SU-8 photolithography. Wet development can be based on at least three different types of exposure-induced changes: variation in molecular weight of the polymers (by cross-linking or by chain scission), reactivity change, and polarity change (Le Barny, 1987). The development of SU-8 patterns exploits the variation in molecular weight of the cross-linked polymer. During the development of SU-8, those areas that were not cross-linked dissolve upon immersion in PGMEA (sold by MicroChem as SU-8 developer). Constant agitation during development is recommended to constantly feed fresh developer to the resist pattern and decrease developing times, but care must be taken when developing high-aspect-ratio structures, as excessive agitation can cause mechanical breakage. In general, microfluidic devices do not have high aspect ratios but instead have a large-area surface that makes them more robust to mechanical breakage and shortens developing times. Agitation can be conducted manually or with a rotator and may be assisted by the application of thermal energy to the developer bath. An alternative to mechanical agitation is the use of a sonicator bath. The use of megasonic frequencies instead of ultrasonic ones proves beneficial in the development of high-aspect-ratio structures and patterns with large surface area such as those shown in [Figure 8.8](#). An important distinction between the two sonication methods is that the higher megasonic frequencies (800–2000 kHz) do not cause the violent cavitation effects found with ultrasonic frequencies (15–400 kHz). This significantly reduces or eliminates cavitation erosion that can lead to pattern fracture and structure debonding from the substrate (Williams et al., 2004a).

The replacement of PGMEA by a liquid with lower surface tension is recommended for the prevention of structure collapse during the resist-drying process. This step is crucial when developing high-aspect-ratio structures (HARS) with high-aspect-ratio gaps in between them; that is, densely packed tall, narrow structures. An example of such structures in microfluidics is the fabrication of very dense arrays of tall pillars to act as physical filters or to increase the area of a functionalized surface in microfluidic applications, exploiting the specific binding of two entities (proteins, DNA, etc.). Stiction forces developed in narrow gaps are strong enough to bend and join SU-8 patterns together during drying as shown in [Figure 8.9](#). More examples of this problem are given by Wang et al. (2005). Although rinsing with isopropyl alcohol (IPA) is the most common method to reduce the surface forces arising during drying, perfluorohexane rinse has also been suggested (Yamashita, 1996). As the gap between the HARS decreases below a few micrometers, other methods must be

**FIGURE 8.9**

Example of SU-8 posts joined together by stiction forces.

used, such as freeze-drying (Tanaka et al., 1993a) and supercritical drying (Namatsu et al., 2000; Jincao et al., 2001). In a supercritical liquid, the surface tension becomes negligible and the capillary force that causes pattern stiction is nonexistent. One example of commercial supercritical drying systems is the Tousimis Samdri[®] line (www.tousimis.com). Theoretical modeling can take into account the Young's modulus of SU-8 and the immersion fluid's surface tension to optimize the cross section, aspect ratio, and packing density of the pattern to avoid stiction (Tanaka et al., 1993b; Jincao et al., 2001; Vora et al., 2005).

8.14 Descumming and Hard Baking

A mild oxygen plasma treatment, so-called *descumming*, removes unwanted resist left behind after development. Negative resists such as SU-8 leave a thin polymer film at the resist–substrate interface and on the pattern surface, which is most likely due to the solid saturation of the used developer (Zaouk, 2008) and can introduce an unexpected change in the surface properties of the SU-8 microfluidics device. An alternative to oxygen plasma is a short dip immersion in acetone. SU-8 withstands acetone when fully polymerized; otherwise, the surface of the pattern will noticeably degrade.

Hard baking removes any casting solvent residues and anneals a resist film that has been weakened either by developer penetration along the resist–substrate interface or by swelling of the resist. Hard baking also improves the hardness of the film and avoids solvent bursts during vacuum processing (Melai et al., 2008). Improved hardness increases the resistance of the resist to subsequent etching steps and makes it less prone to swelling caused by chemicals/buffers that can be used in microfluidic applications. Hard baking frequently occurs at higher temperatures (120°C–150°C) and for longer times than soft baking. Fully cross-linked SU-8 has a glass transition temperature, T_g , that exceeds 200°C,

which makes reflow of the resist practically impossible. A hard bake induces further stress in the pattern and can be omitted from the photolithography process depending on the final application of the SU-8 structure.

8.15 Resist Stripping or Removal

Although this chapter is geared toward the use of SU-8 patterns as molds or structural elements for microfluidic and nanofluidic applications, the following section is an overview of available methods for SU-8 photoresist stripping. The reader may find it useful for the use of SU-8 as a sacrificial material or for the removal of SU-8 from substrates intended to be recycled.

Photoresist stripping, in slightly oversimplified terms, is organic polymer etching. When using the photoresist as sacrificial material, the primary consideration is complete removal of the photoresist without damaging the device under construction. SU-8 photoresist is effectively stripped off with a strong acid such as H_2SO_4 or an acid-oxidant combination such as $\text{H}_2\text{SO}_4\text{-Cr}_2\text{O}_3$ or Piranha (detailed under substrate cleaning), attacking the photoresist but not silicon, silicon oxide, or glass. Other liquid strippers include organic solvent strippers (such as Remover PG from MicroChem and SRGM-Red Stripper from Gersteltec), alkaline strippers (with or without oxidants), and even acetone. These strippers can be used if the postexposure bake is not too long or occurs at a low enough temperature such that solvent molecules are still present in the polymer matrix and act as weak points for the stripper to attack. A hard bake is not recommended if SU-8 is to be removed. High temperatures or long baking times cause the resist to develop a tough "skin," prevent attack from common strippers, and force a removal step using oxygen plasma.

Dry stripping or oxygen plasma stripping, also known as ashing, has become more popular as it poses fewer disposal problems with toxic, flammable, and dangerous chemicals. Wet stripping solutions lose potency in use, causing stripping rates to change with time. Accumulated contamination in solutions can be a source of particles, and liquid phase surface tension and mass transport tend to make photoresist removal difficult and uneven. Dry stripping is more controllable than liquid stripping, less corrosive with respect to metal features on the wafer, and more importantly, it leaves a cleaner surface under the right conditions. Finally, it does not cause the undercutting and broadening of photoresist features, which can be caused by wet strippers.

In solid-gas resist stripping, a volatile product forms either through reactive plasma stripping (e.g., with oxygen), gaseous chemical reactants (e.g., ozone), and radiation (UV) or a combination thereof (e.g., UV/ozone-assisted). Plasma stripping uses a low-pressure electrical discharge to split molecular oxygen (O_2) into its more reactive atomic form (O). This atomic oxygen converts an organic photoresist into a gaseous product that may be pumped away. This type of plasma stripping belongs to the category of chemical dry stripping and is isotropic in nature. In ozone strippers, ozone, at atmospheric pressure, attacks the resist. In UV/ozone stripping, UV helps to break bonds in the resist, paving the way for a more efficient attack by ozone. Ozone strippers have the advantage that no plasma damage can occur on the devices in the process. Reactive plasma stripping is currently the predominant commercial technology because of its high removal rate and throughput. Some different stripper configurations are barrel reactors, downstream strippers, and parallel plate systems.

8.16 Conclusion

The versatility of SU-8 has positioned it as one of the most important materials in polymer microfabrication. Microfluidics benefits from SU-8 photolithography in the batch fabrication of structures of high aspect ratio and/or large surface area, which can range in size from a few millimeters down to tens of nanometers. The good mechanical and excellent chemical properties of cross-linked SU-8 yield polymer microfluidics devices that can handle a variety of samples such as blood, urine, milk, and so forth, as well as buffers and cleaning agents at a wide range of flow pressures and working temperatures. SU-8 has a high transparency for light at wavelengths more than 400 nm and allows for the use of fluorescence and other visualization and detection techniques that are common in microfluidics. The recent commercial introduction of SU-8 with dyes and nanoparticles incorporated in it further enlarges the potential of this photoresist in microfluidics and other applications. SU-8 photolithography yields or supports the fabrication of research devices that are applied in a variety of fields including optics, precision mechanics, energy, and space. Furthermore, complex carbon microstructures can be derived by pyrolyzing SU-8 patterns, a technique known as carbon MEMS (Wang et al., 2005).

Although general guidelines for carrying out SU-8 photolithography exist, significant practical experience is still required to develop successful new SU-8 applications. A generic guideline for SU-8 processing is not really possible because the parameters must always be finely tweaked depending on the available equipment and facilities, the specific application, and most importantly, the geometry of the pattern. Even process parameters once thought trivial are still subjected to further optimization, for example, soft baking time, temperature, and method of baking. Perhaps the most important variable to control in the SU-8 structure manufacturing process is the internal stress. The introduction of thermally induced stresses significantly degrades the final product. Crack formation, bending, and debonding from the substrate can all be minimized by controlled thermal management that includes the use of appropriate heating and cooling ramps. However, baking techniques and procedures must be optimized to eliminate long heating ramps and relaxation times between processing steps. The use of polymer substrates with thermal properties similar to that of SU-8 proves beneficial to minimize thermal stresses induced during baking. Moreover, polymer substrates are less expensive and significantly less brittle when compared with silicon and glass. Alternatives to traditional SU-8 processing include the use of SU-8 dry films for lamination. This approach eliminates the casting solvent from the photoresist formulation, reduces process time significantly, especially when working with thick layers ($>200\ \mu\text{m}$), and can make SU-8 photolithography a roll-to-roll process. The constant optimization of process methodologies, techniques, and equipment has enabled a steady improvement of SU-8 photolithography, and hopefully, this will eventually result in the application of SU-8 photolithography in a number of commercial devices rather than just in research tools.

Acknowledgments

The authors thank Rob Hardman from MicroChem for useful discussions regarding SU-8 formulations.

References

- Abgrall P, Charlot S, Fulcrand R, Paul L, Boukabache A, Gué A. (2008). Low-stress fabrication of 3D polymer free standing structures using lamination of photosensitive films. *Microsyst Technol.* 14:1205–14.
- Abgrall P, Conedera V, Camon H, Gue A, Nguyen N. (2007). SU-8 as a structural material for labs-on-chips and microelectromechanical systems. *Electrophoresis.* 28:4539–51.
- Abgrall P, Lattes C, Conédéra V, Dollat X, Colin S, Gué AM. (2006). A novel fabrication method of flexible and monolithic 3D microfluidic structures using lamination of SU-8 films. *J Micromech Microeng.* 16:113–21.
- Acrivos A, Shah MJ, Petersen EE. (1960). On the flow of a non-Newtonian liquid on a rotating disk. *J Appl Phys.* 31(6):963–8.
- Agirregabiria M, Blanco FJ, Berganzo J, Arroyo MT, Fullaondo A, Mayora K, et al. (2005). Fabrication of SU-8 multilayer microstructures based on successive CMOS compatible adhesive bonding and releasing steps. *Lab Chip.* 5:545–52.
- Aktary M, Jensen MO, Westra KL, Brett MJ, Freeman MR. (2003). High-resolution pattern generation using the epoxy novolak SU-8 2000 resist by electron beam lithography. *J Vac Sci Technol B.* 21(4):L5–7.
- Anderson JR, Chiu DT, Jackman RJ, Cherniavskaya O, McDonald JC, Wu H, et al. (2000). Fabrication of topologically complex three-dimensional microfluidic systems in PDMS by rapid prototyping. *Anal Chem.* 72:3158–64.
- Andersson H, van den Berg A. (2003). Microfluidic devices for celloamics: a review. *Sens Actuators B Chem.* 92(3):315–25.
- Angelo R, Gelorme J, Kucynski J, Lawrence W, Pappas S, Simpson L. (1992). *Photocurable epoxy composition with sulfonium salt photoinitiator.* United States patent 5102772. April 7.
- Anhoj TA, Jorgensen AM, Zauner DA, Hubner J. (2006). The effect of soft bake temperature on the polymerization of SU-8 photoresist. *J Micromech Microeng.* 16:1819–24.
- Arnone C. (1992). The laser-plotter: a versatile lithographic tool for integrated optics and microelectronics. *Microelectron Eng.* 17:483–6.
- Auroux P, Iossifidis D, Reyes DR, Manz A. (2002). Micro total analysis systems. II. Analytical standard operations and applications. *Anal Chem.* 74(12):2637–52.
- Bakajin O, Fountain E, Morton K, Chou SY, Sturm JC, Austin RH. (2006). Materials aspects in micro- and nanofluidic systems applied to biology. *MRS Bull.* 31:108–13.
- Barber RL, Ghantasala MK, Divan R, Vora KD, Harvery EC, Mancini DC. (2005). Optimisation of SU-8 processing parameters for deep x-ray lithography. *Microsyst Technol.* 11(4):303–10.
- Barber R, Ghantasala MK, Divan R, Mancini DC, Harvey EC. (2007). Study of stress and adhesion strength in SU-8 resist layers on silicon substrate with different seed layers. *Journal of Micro/Nanolithography, MEMS and MOEMS.* 6(3):033006–8.
- Barker SLR, Ross D, Tarlov MJ, Gaitan M, Locascio LE. (2000a). Control of flow direction in microfluidic devices with polyelectrolyte multilayers. *Anal Chem.* 72(24):5925–9.
- Barker SLR, Tarlove MJ, Canavan H, Hickman JJ, Locascio LE. (2000b). Plastic microfluidic devices modified with polyelectrolyte multilayers. *Anal Chem.* 72(20):4899–903.
- Bassous E, Taub HH, Kuhn L. (1977). Ink jet printing nozzle arrays etched in silicon. *Appl Phys Lett.* 31:135–7.
- Becker H, Gartner C. (2000). Polymer microfabrication methods for microfluidic analytical applications. *Electrophoresis.* 21(1):12–26.
- Becker H, Locascio LE. (2002). Polymer microfluidic devices. *Talanta.* 56(2):267–87.
- Beebe DJ, Mensing GA, Walker GM. (2002). Physics and applications of microfluidics in biology. *Ann Rev Biomed Eng.* 4:261–86.
- Berdichevsky Y, Khandurina J, Guttman A, Lo Y. (2004). UV/ozone modification of poly(dimethylsiloxane) microfluidic channels. *Sens Actuators B Chem.* 97(2–3):402–8.

- Bertsch A, Lorenz H, Renaud P. (1999a). 3D microfabrication by combining microstereolithography and thick resist UV lithography. *Sens Actuators A Phys.* 73:14–23.
- Bertsch A, Lorenz H, Renaud P. (1999b). 3D microfabrication by combining microstereolithography and thick resist UV lithography. *Sens Actuators A Phys.* 73(1–2):14–23.
- Beuret C, Racine G, Gobet J, Luthier R, de Rooji NF. (1994). Microfabrication of 3D multidirectional inclined structures by UV lithography and electroplating. Paper presented at 17th International Conference on MEMS, MEMS '94, Oiso, Japan.
- Bilenberg B, Jacobsen S, Schmidt MS, Skjolding LHD, Shi P, Bøggild P, et al. (2006). High resolution 100 kV electron beam lithography in SU-8. *Microelectron Eng.* 83(4–9):1609–12.
- Boedeker Plastics, Inc. (2009a). PEEK (PolyEtherEtherKetone) specifications [cited July 31, 2009]. Available from: http://www.boedeker.com/peek_p.htm.
- Boedeker Plastics, Inc. (2009b). Polycarbonate specifications [cited July 31, 2009]. Available from: http://www.boedeker.com/polyc_p.htm.
- Bogdanov AL, Peredkov SS. (2000). Use of SU-8 photoresist for very high aspect ratio x-ray lithography. *Microelectron Eng.* 53(1–4):493–6.
- Chen C, Hirdes D, Folch A. (2003). Gray-scale photolithography using microfluidic photomasks. *Proc Natl Acad Sci USA.* 100(4):1499–504.
- Chen R, Cheng C. (2001). Study of spin coating properties of SU-8 thick-layer photoresist. Paper presented at Advances in Resist Technology and Processing XVIII, Santa Clara, CA.
- Chin CD, Linder V, Sia SK. (2007). Lab-on-a-chip devices for global health: past studies and future opportunities. *Lab Chip.* 7:41–57.
- Chollet F. (2009). SU-8: thick photo-resist for MEMS [cited April 15, 2009]. Available from: <http://memscyclopedia.org/su8.html>.
- Chuang Y, Tseng F, Lin W. (2002). Reduction of diffraction effect of UV exposure on SU-8 negative thick photoresist by air gap elimination. *Microsyst Technol.* 8(4–5):308–13.
- Chung TD, Kim HC. (2007). Recent advances in miniaturized microfluidic flow cytometry for clinical use. *Electrophoresis.* 28(24):4511–20.
- Cirlex. [cited 2009 Apr 15]. Available from: <http://www.matweb.com>.
- Craighead H. (2006). Future lab-on-a-chip technologies for interrogating individual molecules. *Nature.* 442:387–93.
- Crivello JV. (2000). The discovery and development of onium salt cationic photoinitiators. *J Polym Sci A Polym Chem.* 37(23):4241–54.
- Crivello JV, Lam JHW. (1977). Diaryliodonium salts. A new class of photoinitiators for cationic polymerization. *Macromolecules.* 10(6):1307–15.
- Crivello JV, Lam JHW. (1979). Photoinitiated cationic polymerization with triarylsulfonium salts. *J Polym Sci.* 17:977–99.
- Crivello JV, Lam JHW. (1980). Complex triarylsulfonium salt photoinitiators. I. the identification, characterization, and syntheses of a new class of tryarylsulfonium salt photoinitiators. *J Polym Sci A Polym Chem.* 18:2677–95.
- Dai W, Lian K, Wang W. (2005). A quantitative study on the adhesion property of cured SU-8 on various metallic surfaces. *Microsyst Technol.* 11:526–34.
- del Campo A, Greiner C. (2007). SU:8 a photoresist for high-aspect-ratio and 3D submicron lithography. *J Micromech Microeng.* 17:R81–95.
- Dentinger PM, Clift WM, Goods SH. (2002). Removal of SU-8 photoresist for thick film applications. *Microelectron Eng.* 61–62:993–1000.
- Deubel M, von Freymann G, Wegener M, Pereira S, Busch K, Soukoulis CM. (2004). Direct laser writing of three-dimensional photonic-crystal templates for telecommunications. *Nat Mater.* 3(7):444–7.
- Dittrich PS, Manz A. (2006). Lab-on-a-chip: microfluidics in drug discovery. *Nat Rev Drug Discov.* 5:210–8.
- Dittrich PS, Tachikawa K, Manz A. (2006). Micro total analysis systems. latest advancements and trends. *Anal Chem.* 78(12):3887–907.
- Duffy DC, McDonald JC, Schueller OJA, Whitesides GM. (1998a). Rapid prototyping of microfluidic systems in poly(dimethylsiloxane). *Anal Chem.* 70:4974–84.

- Duffy DC, McDonald JC, Schueller OJA, Whitesides GM. (1998b). Rapid prototyping of microfluidic systems in poly(dimethylsiloxane). *Anal Chem.* 70(23):4974–84.
- Dyer CK. (2002). Fuel cells for portable applications. *J Power Sources.* 106:31–4.
- Emslie AG, Bonner FT, Peck LG. (1959). Flow of a viscous liquid on a rotating disk. *J Appl Phys.* 29(5):858–62.
- Erdler G, Frank M, Lehmann M, Reinecke H, Muller C. (2006). Chip integrated fuel cell. *Sens Actuators A Phys.* 132:331–6.
- Feng R, Farris RJ. (2003). Influence of processing conditions on the thermal and mechanical properties of SU8 negative photoresist coatings. *J Micromech Microeng.* 13:80–8.
- Figeys D, Pinto D. (2000). Lab-on-a-chip: a revolution in biological and medical sciences. *Anal Chem.* 72(9):330 A, 335 A.
- Fiorini GS, Chiu DT. (2005). Disposable microfluidic devices: fabrication, function, and application. *Biotechniques.* 38(3):429–46.
- FLUOROTHERM Polymers, Inc. (2009). PTFE characteristics and behavior. [cited July 31, 2009]. Available from: http://www.fluorotherm.com/ptfe_properties.html.
- Gelorme JD, Cox RJ, Gutierrez SAR. (1989). *Photoresist composition and printed circuit boards and packages made therewith*. Patent 4882245. November 21.
- Gersborg-Hansen M, Kristensen A. (2006). Optofluidic third order distributed feedback dye laser. *Appl Phys Lett.* 89:103518–0,103518–3.
- Giancoli DC. (1998). *Physics, Principles with Applications*. 5th ed. New Jersey: Prentice Hall.
- Gravesen P, Branebjerg J, Jensen OS. (1993). Microfluidics—a review. *J Micromech Microeng.* 3:168–82.
- Guerin LJ. (2005). The SU8 homepage [cited July 30, 2009]. Available from: <http://www.geocities.com/guerinlj/>.
- Han M, Lee W, Lee S, Lee SS. (2004). 3D microfabrication with inclined/rotated UV lithography. *Sens Actuators A Phys.* 111:14–20.
- Harris TW. (1976). *Chemical Milling*. Oxford: Clarendon Press.
- Henry AC, Tutt TJ, Galloway M, Davidson YY, McWhorter S, Soper SA, McCarley RL. (2000). Surface modification of poly(methyl methacrylate) used in the fabrication of microanalytical devices. *Anal Chem.* 72(21):5331–7.
- Henry AC, Waddell EA, Shreiner R, Locascio LE. (2002). Control of electroosmotic flow in laser-ablated and chemically modified hot imprinted poly(ethylene terephthalate glycol) microchannels. *Electrophoresis.* 23:791–8.
- Hirai Y, Inamoto Y, Sugano K, Tsuchiya T, Tabata O. (2007). Moving mask UV lithography for three-dimensional structuring. *J Micromech Microeng.* 17:199–206.
- Hu G, Li D. (2007). Multiscale phenomena in microfluidics and nanofluidics. *Chem Eng Sci.* 62(13):3443–54.
- Hull R. (1999). *Properties of Crystalline Silicon*. London: The Institution of Engineering and Technology.
- Hung K, Hu H, Tseng F. (2004). Application of 3D glycerol-compensated inclined-exposure technology to an integrated optical pick-up head. *J Micromech Microeng.* 14:975–83.
- Hung K, Tseng F, Chou H. (2005). Application of 3D gray mask for the fabrication of curved SU-8 structures. *Microsyst Technol.* 11:365–9.
- Ito H. (1996). Chemical amplification resists: history and development within IBM. *IBM J Res Dev.* 41:69–80.
- Iverson BD, Garimella SV. (2008). Recent advances in microscale pumping technologies: a review and evaluation. *Microfluid Nanofluidics.* 5:145–74.
- Janasek D, Franzke J, Manz A. (2006). Scaling and the design of miniaturized chemical-analysis systems. *Nature.* 442:374–80.
- Jankowski AF, Hayes JP, Graff RT, Morse JD. (2002). Micro-fabricated thin film fuel cells for portable power requirements. *Mater Res Soc Symp Proc.* 730:93–8.
- Jensen KF. (2006). Silicon-based microchemical systems: characteristics and applications. *MRS Bull.* 31:101–7.

- Jincao Y, Matthews MA. (2001). Prevention of photoresist pattern collapse by using liquid carbon dioxide. *Ind Eng Chem Res.* 40(24):5858–60.
- Kapton Polyimide Film. [cited 2009 Apr 15]. Available from: http://www2.dupont.com/Kapton/en_US/.
- Kim K, Park DS, Lu HM, Che W, Kim K, Lee J, et al. (2004). A tapered hollow metallic microneedle array using backside exposure of SU-8. *J Micromech Microeng.* 14:597–603.
- King JW, Williams LL. (2003). Utilization of critical fluids in processing semiconductors and their related materials. *Curr Opin Solid State Mater Sci.* 7(4–5):413–24.
- Kirby BJ, Hasselbrink EF Jr. (2004a). Zeta potential of microfluidic substrates: I. Theory, experimental techniques, and effects on separations. *Electrophoresis.* 25:187–202.
- Kirby BJ, Hasselbrink EF Jr. (2004b). Zeta potential of microfluidic substrates: II. Data for polymers. *Electrophoresis.* 25:203–13.
- Kjeang E, Djilali N, Sinton D. (2009). Microfluidic fuel cells: a review. *J Power Sources.* 186:353–69.
- Koller DM, Galler N, Ditzbacher H, Hohenau A, Leitner A, Aussenegg FR, et al. (2009). Direct fabrication of micro/nano fluidic channels by electron beam lithography. *Microelectron Eng.* 86(4–6):1314–6.
- Kuriyama N, Kubota T, Okamura D, Suzuki T, Sasahara J. (2008). Design and fabrication of MEMS-based monolithic fuel cells. *Sens Actuators A Phys.* 145–146:354–62.
- Le Barny P. (1987). *Molecular Engineering of Ultrathin Polymeric Films*. Stroeve P, Franses E, editors. New York: Elsevier; pp. 99–150.
- Lee KY, LaBianca N, Rishton SA, Zolgharnain S, Gelorme JD, Shaw J, et al. (1995). Micromachining applications of a high resolution ultrathick photoresist. *J Vac Sci Technol B.* 13:3012–6.
- Lee SJ, Shi W, Maciel P, Cha SW. Boise (ID); 2003.
- Levinson HJ. (2005). *Principles of Lithography*. 2nd ed. Bellingham (WA): SPIE Publications.
- Li B, Liu M, Chen Q. (2005). Low-stress ultra-thick SU-8 UV photolithography process for MEMS. *J Microlithogr Microfabr Microsyst.* 4(4):043008–1, 043008–6.
- Lin C, Lee G, Chang B, Chang G. (2002). A new fabrication process for ultra-thick microfluidic microstructures utilizing SU-8 photoresist. *J Micromech Microeng.* 12:590–7.
- Linder V, Verpoorte E, Thormann W, de Rooji NF, Sigrist H. (2001). Surface biopassivation of replicated poly(dimethylsiloxane) microfluidic channels and application to heterogeneous immunoreaction with on-chip fluorescence detection. *Anal Chem.* 73(17):4181–9.
- Ling ZG, Lian K, Jian L. (2000). Improved patterning quality of SU-8 microstructures by optimizing the exposure parameters. Paper presented at Advances in Resist Technology and Processing XVIII, Santa Clara, CA.
- Liu Y, Fanguy JC, Bledsoe JM, Henry CS. (2000). Dynamic coating using polyelectrolyte multilayers for chemical control of electroosmotic flow in capillary electrophoresis microchips. *Anal Chem.* 72(24):5939–44.
- Lorentz H, Despont M, Fahrni N, Brugger J, Vettiger P, Renaud P. (1998). High-aspect-ratio, ultra-thick, negative-tone near-UV photoresist and its applications for MEMS. *Sens Actuators A Phys.* 64:33–9.
- Lorenz H, Despont M, Fahrni M, LaBianca N, Vettiger P, Renaud P. (1997). SU-8: a low-cost negative resist for MEMS. *J Micromech Microeng.* 7:121.
- Lü C, Yin X, Wang M. (2007). Fabrication of high aspect ratio metallic microstructures on ITO glass substrate using reverse-side exposure of SU-8. *Sens Actuators A Phys.* 136(1):412–6.
- Madou MJ. (2009). *Manufacturing Techniques for Microfabrication and Nanotechnology*. 1st ed. Boca Raton (FL): CRC Press.
- Madou M, Florkey J. (2000). From batch to continuous manufacturing of biomedical devices. *Chem Rev.* 100:2679–91.
- Manz A, Graber N, Widmer HM. (1990). Miniaturized total chemical analysis systems: a novel concept for chemical sensing. *Sens Actuators.* B1:244–8.
- Martinez-Duarte R. (2009). Fabrication of carbon micro molds. Master of Science in Mechanical and Aerospace Engineering. Irvine: University of California.

- Martinez-Duarte R, Madou MJ, Kumar G, Schroers J. (2009). A novel method for amorphous metal micromolding using carbon MEMS. Paper presented at 15th International Conference on Solid-State Sensors, Actuators & Microsystems, Transducers 2009, Denver, CO.
- Mata A, Fleischman AJ, Roy S. (2005). Characterization of polydimethylsiloxane (PDMS) properties for biomedical micro/nanosystems. *Biomed Microdevices*. 7(4):281–93.
- McHardy J, Haber SP, editors. (1998). Supercritical fluid cleaning: Fundamentals, technology and applications. In: *Materials Science and Process Technology*. Westwood (NJ): Noyes Publications.
- Melai J, Salm C, Wolters R, Schmitz J. (2008). Qualitative and quantitative characterization of outgassing from SU-8. *Microelectron Eng*. 86(4–6):761–4.
- MEMS Exchange. (2009). Silicon dioxide (SiO₂), film [cited July 31, 2009]. Available from: <http://www.memsnet.org/material/silicondioxidesio2film/>.
- Metz TE, Savage RN, Simmons HO. (1992). In situ control of photoresist coating processes. *Semiconductor Int*. 15:68–9.
- MicroChem Corp. (2009). SU-8 2000 permanent epoxy negative photoresist processing guidelines. [cited April 12, 2009]. Available from: www.microchem.com.
- Mijatovic D, Eijkel JCT, van den Berg A. (2005). Technologies for nanofluidic systems: top–down vs. bottom–up—a review. *Lab Chip*. 5:492–500.
- Mitchell P. (2001). Microfluidics—downsizing large-scale biology. *Nat Biotechnol*. 19:717–21.
- Moreau WM. (1987). *Semiconductor Lithography: Principles, Practices and Materials*. New York: Springer.
- Morse JD. (2007). Micro-fuel cell power sources. *Int J Energy Res*. 31(6):576–602.
- Mylar Technical Information. [cited 2009 Apr 16]. Available from: <http://usa.dupontteijinfilms.com/informationcenter/technicalinfo.aspx>.
- Nallani AK, Park SW, Lee JB. (2003). Characterization of SU-8 as a photoresist for electron-beam lithography. Paper presented at Smart Sensors, Actuators, and MEMS, Maspalomas, Gran Canaria, Spain.
- Namatsu H, Yamazaki K, Kurihara K. (2000). Supercritical resist dryer. *J Vac Sci Technol B*. 18(2):780–4.
- Nguyen N, Chan SH. (2006). Micromachined polymer electrolyte membrane and direct methanol fuel cells—a review. *J Micromech Microeng*. 16:R1–12.
- Nordstrom M, Marie R, Calleja M, Boisen A. (2004). Rendering SU-8 hydrophilic to facilitate use in micro channel fabrication. *J Micromech Microeng*. 14:1614–7.
- Nordström M, Johansson A, Noguerón ES, Clausen B, Calleja M, Boisen A. (2005). Investigation of the bond strength between the photo-sensitive polymer SU-8 and gold. *Microelectron Eng*. 78–79:152–7.
- PDMS (polydimethylsiloxane). [cited 2009 Jul 31]. Available from: <http://web.mit.edu/6.777/www/matprops/pdms.htm>.
- Pépin A, Studer V, Decanini D, Chen Y. (2004). Exploring the high sensitivity of SU-8 resist for high resolution electron beam patterning. *Microelectron Eng*. 73–74:233–7.
- Peterman MC, Huie P, Bloom DM, Fishman HA. (2003). Building thick photoresist structures from the bottom up. *J Micromech Microeng*. 13:380–2.
- Petersen KE. (1979). Fabrication of an integrated, planar silicon ink-jet structure. *IEEE Trans Electron Devices*. ED-26(12):1918–20.
- Pugmire DL, Waddell EA, Haasch R, Tarlov MJ, Locascio LE. (2002). Surface characterization of laser-ablated polymers used for microfluidics. *Anal Chem*. 74(4):871–8.
- Reyes DR, Iossifidis D, Aurox P, Manz A. (2002). Micro total analysis systems. I. Introduction, theory and technology. *Anal Chem*. 74(12):2623–36.
- Reznikova EF, Mohr J, Hein H. (2005). Deep photo-lithography characterization of SU-8 resist layers. *Microsyst Technol*. 11:282–91.
- Reznikova E, Mohr J, Boerner M, Nazmov V, Jakobs P. (2008). Soft x-ray lithography of high aspect ratio SU8 submicron structures. *Microsyst Technol*. 14(9–11):1683–8.
- Robinson APG, Zaid HM, Gibbons FP, Palmer RE, Manickam M, Preece JA, et al. (2006). Chemically amplified molecular resists for electron beam lithography. *Microelectron Eng*. 83(4–9):1115–8.

- Ruhmann R, Ahrens G, Schuetz A, Voskuhl J, Gruetzner G. (2001). Reduction of internal stress in SU-8-like negative tone photoresist for MEMS applications by chemical modification. Paper presented at Advances in Resist Technology and Processing XVIII, Santa Clara, CA.
- Sato H, Kakinuma T, Go JS, Shoji S. (2004a). In-channel 3-D micromesh structures using maskless multi-angle exposures and their microfilter application. *Sens Actuators A Phys.* 111(1):87–92.
- Schwartz LW, Valery R. (2004). Theoretical and numerical results for spin coating of viscous liquids. *Phys Fluids.* 16(3):569–84.
- Shaw JM, Gelorme JD, LaBianca NC, Conley WE, Holmes SJ. (1997). Negative photoresists for optical lithography. *IBM J Res Dev.* 41:81–94.
- Shaw M, Nawrocki D, Hurditch R, Johnson D. (2003). Improving the process capability of SU-8. *Microsyst Technol.* 10:1–6.
- Shew B, Huang T, Liu K, Chou C. (2004). Oxygen quenching effect in ultra-deep x-ray lithography with SU-8 resist. *J Micromech Microeng.* 14:410–4.
- Sikanen T, Tuomikoski S, Ketola RA, Kostianen R, Franssila S, Kotiaho T. (2005). Characterization of SU-8 for electrokinetic microfluidic applications. *Lab Chip.* 5:888–96.
- Song Y, Kumar CSSR, and Hormes J. (2004). Fabrication of an SU-8 based microfluidic reactor on a PEEK substrate sealed by a ‘flexible semi-solid transfer’ (FST) process. *J Micromech Microeng.* 14:932–40.
- Squires TM, Quake SR. (2005). Microfluidics: fluid physics at the nanoliter scale. *Rev Mod Phys.* 77:977–1026.
- Stauffer JM, Oppliger Y, Regnault P, Baraldi L, Gale MT. (1992). Electron beam writing of continuous resist profiles for optical applications. *J Vac Sci Technol B.* 10:2526.
- Stone HA, Stroock AD, Ajdari A. (2004). Engineering flows in small devices: microfluidics toward a lab-on-a-chip. *Annu Rev Fluid Mech.* 36:318–411.
- Stroock AD, Cabodi M. (2006). Microfluidic biomaterials. *MRS Bull.* 31:114–9.
- Sure A, Dillon T, Murakowski J, Lin C, Pustai D, Prather DW. (2003). Fabrication and characterization of three-dimensional silicon tapers. *Optics Express.* 11:3555–61.
- Taff J, Kashte Y, Spinella-Mamo V, Paranjape M. (2006). Fabricating multilevel SU-8 structures in a single photolithographic step using colored masking patterns. *J Vac Sci Technol A.* 24(3):742–6.
- Tan TL, Wong D, Lee P, Rawat RS, Springham S, Patran A. (2006). Characterization of chemically amplified resist for x-ray lithography by fourier transform infrared spectroscopy. *Thin Solid Films.* 504(1–2):113–6.
- Tanaka T, Mitsuaki M, Hiroaki O, Taro O. (1993a). Freeze-drying process to avoid resist pattern collapse. *Jpn J Appl Phys.* 32(12R):5813–4.
- Tanaka T, Morigami M, Atoda N. (1993b). Mechanism of resist pattern collapse during development process. *Jpn J Appl Phys.* 32:6059–64.
- Tangram Technology Ltd. (2005). Polymethyl methacrylate—PMMA (acrylic) polymer data sheet [cited July 31, 2009]. Available from: <http://www.tangram.co.uk/TI-Polymer-PMMA.html>.
- Terry SC, Jerman JH, Angell JB. (1979). A gas chromatographic air analyzer fabricated on a silicon wafer. *IEEE Trans Electron Devices.* ED-26:1880–6.
- Thompson LF. (1994). An introduction to lithography. In: Thompson LF, Willson CG, Bowden MJ, editors. *Introduction to Microlithography*. 2nd ed. Washington (DC): American Chemical Society; pp. 1–17.
- Tuckerman DB, Pease RF. (1981). High-performance heat sinking for VLSI. *IEEE Electron Device Lett.* ED-2:126–9.
- Ullal CK, Maldovan M, Thomas EL. (2004). Photonic crystals through holographic lithography: simple cubic, diamond-like, and gyroid-like structures. *Appl Phys Lett.* 84:5434–6.
- van Kan JA, Sanchez JL, Xu B, Osipowicz T, Watt F. (1999). Micromachining using focused high energy ion beams: deep ion beam lithography. *Nucl Instrum Methods Phys Res B.* 148:1085–9.
- Verpoorte E. (2002). Microfluidic chips for clinical and forensic analysis. *Electrophoresis.* 23:677–712.
- Verpoorte E, De Rooji NF. (2003). Microfluidics meets MEMS. *Proc IEEE.* 91(6):930–53.
- Vilkner T, Janasek D, Manz A. (2004). Micro total analysis systems. Recent developments. *Anal Chem.* 76(12):3373–86.

- Vora KD, Shew BY, Harvey EC, Hayes JP, Peele AG. (2005). Specification of mechanical support structures to prevent SU-8 stiction in high aspect ratio structures. *J Micromech Microeng.* 15:978–83.
- Vrentas JS, Duda JL. (1977a). Diffusion in polymer-solvent systems. I. Reexamination of the free-volume theory. *J Polym Sci B.* 15:403–16.
- Vrentas JS, Duda JL. (1977b). Diffusion in polymer-solvent systems. II. A predictive theory for the dependence of diffusion coefficients on temperature, concentration, and molecular weight. *J Polym Sci B.* 15:417–39.
- Wang C, Jia G, Taherabadi LH, Madou MJ. (2005). A novel method for the fabrication of high-aspect ratio C-MEMS structures. *J Microelectromech Syst.* 14(2):348–58.
- Wang SC, Perso CE, Morris MD. (2000). Effects of alkaline hydrolysis and dynamic coating on the electroosmotic flow in polymeric microfabricated channels. *Anal Chem.* 72(7):1704–6.
- Wang X, Cheng C, Wang S, Liu S. (2009). Electroosmotic pumps and their applications in microfluidic systems. *Microfluid Nanofluidics.* 6:145–62.
- Washo BD. (1977). Rheology and modeling of the spin coating process. *IBM J Res Dev.* March:190–98.
- Weigl BH, Bardell RL, Cabrera CR. (2003). Lab-on-a-chip for drug development. *Adv Drug Deliv Rev.* 55(3):349–77.
- Whitesides GM. (2006). The origins and the future of microfluidics. *Nature.* 442:368–73.
- Williams JD, Wang W. (2004a). Using megasonic development of SU-8 to yield ultra-high aspect ratio microstructures with UV lithography. *Microsyst Technol.* 10:694–8.
- Williams JD, Wang W. (2004b). Study on the postbaking process and the effects on UV lithography of high aspect ratio SU-8 microstructures. *J Microlithogr Microfabr Microsyst.* 3:563–8.
- Windt DL, Cirelli RA. (1999). Amorphous carbon films for use as both variable-transmission apertures and attenuated phase shift masks for deep ultraviolet lithography. *J Vac Sci Technol B.* 17:930–2.
- Wolf S, Tauber RN. (2000). *Silicon Processing for the VLSI Era.* Sunset Beach: Lattice Press.
- Wu C, Chen M, Tseng F. (2003). *SU-8 Hydrophilic Modification by Forming Copolymer with Hydrophilic Epoxy Molecule.* Squaw Valley, CA.
- Xia Y, Whitesides GM. (1998). Soft lithography. *Annu Rev Mater Sci.* 28:153–84.
- Yamashita Y. (1996). Sub-0.1 μm patterning with high aspect ratio of 5 achieved by preventing pattern collapse. *Jpn J Appl Phys.* 35:2385–6.
- Yang R, Wang W. (2005). A numerical and experimental study on gap compensation and wavelength selection in UV-lithography of ultra-high aspect ratio SU-8 microstructures. *Sens Actuators B Chem.* 110(2):279–88.
- Yoon Y, Park J, Allen MG. (2006). Multidirectional UV lithography for complex 3-D MEMS structures. *J Microelectromech Syst.* 15(5):1121–30.
- Yu H, Li B, Zhang X. (2006). Flexible fabrication of three-dimensional multi-layered microstructures using a scanning laser system. *Sens Actuators A Phys.* 125:553–64.
- Zaouk RB. (2008). Carbon MEMS from the nanoscale to the macroscale: novel fabrication techniques and applications in electrochemistry. PhD in Mechanical and Aerospace Engineering, Irvine: University of California.
- Zdeblick MJ, Bartha PW, Angell JA. (1986). Microminiature fluidic amplifier. In: *Technical Digest of the IEEE Solid-State Sensor and Actuator Workshop (Hilton Head Island, SC).* New York: IEEE.
- Zhang J, Chan-Park MB, Conner SR. (2004). Effect of exposure dose on the replication fidelity and profile of very high aspect ratio microchannels in SU-8. *Lab Chip.* 4:646–53.
- Zhang J, Tan KL, Hong GD, Yang LJ, Gong HQ. (2001). Polymerization optimization of SU-8 photoresist and its applications in microfluidic systems and MEMS. *J Micromech Microeng.* 11:20–6.
- Zhang X, Haswell SJ. (2006). Materials matter in microfluidic devices. *MRS Bull.* 31:95–9.